	Co
Low	C
22	Cr
22	Ni
14	W
.08	La

Haynes Alloy No. 188

1 **GENERAL**

Haynes Alloy No. 188 is one of the most widely used cobalt-base sheet alloy in the aircraft engine field. It was first introduced in 1966. The strength of Haynes Alloy No. 188 is similar to that of its predecessor, L-605. However, the oxidation resistance and resistance to aging embrittlement of Haynes Alloy No. 188 are superior. Tensile elongation exceeds 10 percent after aging for up to 1000 hours at 1400 to 1600 F. It has a 100 F creep-rupture strength advantage over Hastelloy X. Cryogenic temperatures do not affect significantly the ductility of the alloy, but strength levels are increased markedly.

The excellent oxidation resistance results from a high chromium level and small additions of lanthanum, which apparently modifies the oxide scale in such a manner that the oxide becomes extremely tenacious and protective when exposed to temperatures through 2000 F.

Haynes Alloy No. 188 has a stabilized face-centered cubic structure which is solid solution strengthened by the addition of 14 percent W. Strengthening is further enhanced by the precipitation of M_6C and $M_{23}C_6$ carbides. Intermediate temperature ductility is achieved by deterring the formation of the embrittling CO_2W Laves type phase through properly balanced composition.

Because of its excellent mechanical properties, oxidation resistance, and weldability, Haynes Alloy No. 188 meets the high temperature material requirements for gas turbine applications as well as many of those in the airframe, nuclear, and chemical fields. Typical uses are as transition ducts, combustor cans, spray bars, flame-holders, and liners in jet engines. The alloy is used also in the space shuttle main engine and is attractive for re-entry heat shield applications (1,30,31,61).

Haynes Alloy No. 188 is covered by U.S. Patent No. 3,418,111 (2).

1.01 **Commercial Designation**
Haynes Alloy No. 188.

1.02 **Alternate Designations**
HS-188, HA-188, and UNS R30188.

1.03 **Specifications**
1.031 AMS 5608 (sheet, strip, and plate).
1.032 AMS 5772 (bars, forgings, and rings).
1.033 AMS 5801 (alloy wire, welding).

1.04 **Composition**
Composition, Table 1.04.

1.05 **Heat Treatment**
1.051 The standard heat treatment is a simple solution treatment consisting of heating to 2125 to 2175 F, holding at heat for a time commensurate with the thickness (but not more than 30 min for sheet, strip, and plate), followed by either water quenching or rapid cooling in air (1,3,4).

1.052 Any thermal treatment following solution heat treatment as given above should not involve use of temperatures higher than 2025 to 2075 F (3).

1.053 For certain applications, the tensile strength of sheet at room and elevated temperatures can be increased by cold rolling followed by aging near 1000 F, 4 to 16 hr. Cold working prior to aging significantly increases the rate of the aging reaction (1).

1.054 Effect of solution treatment and aging on microstructure and microconstituents, Table 1.054.

1.06 **Hardness**

1.061 The hardness of sheet in the solution treated condition is approximately HRC 21 (about 60 to 62 HRA) (1,7).

1.062 AMS 5772 specifies that the hardness of bars shall not exceed BHN 302, and forgings and flash welded rings BHN 293 in the solution treated condition (4).

1.063 Effect of cold rolling on the hardness and yield strength of sheet, Figure 1.063.

1.064 Hardness recovery characteristics for cold rolled sheet upon annealing, Figure 1.064.

1.065 Effect of aging temperature on hardness. Sheet material solution treated to a hardness of HRA 60 and then exposed for 200 to 500 hr at various temperatures in the range of 900 to 1850 F showed only a slight increase in hardness to 61 to 64 HRA with readings of 61 to 62 HRA occurring in the two ranges of 900 to 1200 F and 1800 to 1850 F, and 63 to 64 HRA in the 1300 to 1700 F range (1). Continued exposure thru 6,244 hr results in an additional increase in hardness, especially in the 1300 to 1500 F range (6).

1.066 Effect of elevated temperature exposure on hardness of two heats, Figure 1.066.

1.07 **Forms and Conditions Available**

1.071 The alloy is available in the full commercial range of sizes for sheet and strip, plate, bar, wire, forging billets, forgings, and bare welding rod (7).

1.072 All wrought products are furnished in the solution heat treated (annealed) conditions unless otherwise specified.

1.073 Welding wire is supplied with a cold drawn, bright finish in a temper which will provide proper feeding of the wire in machine welding equipment. Wire is available on spools or in cut lengths for manual welding.

1.08 **Melting and Casting Practice**
Air melt followed by consumable electrode, vacuum arc remelting.

1.09 **Special Considerations**

1.091 Haynes Alloy No. 188 was developed in part to alleviate the susceptibility to aging embrittlement exhibited by its predecessor, L-605. Haynes Alloy No. 188 is successful in this regard in that embrittlement occurs only after longer aging times than with L-605 (see Figure 3.0233). Embrittlement of Haynes Alloy No. 188 is primarily the result of precipitation of CO_2W Laves phase, although precipitation of M_6C and $M_{23}C_6$ carbide phases may contribute also. Tensile ductility is decreased at low

	Co
Low	C
22	Cr
22	Ni
14	W
.08	La

Haynes Alloy No. 188

temperatures after aging. However, ductility of aged material at 1400 to 1800 F is high and approximates that of solution annealed unaged material (see Figures 3.0315 and 3.0316).

To prevent or retard the formation of the embrittling Co_2W Laves phase in the alloy during long-term, elevated temperature exposure, the chemical composition of production heats should be controlled within appropriate limits which result in an average electron-vacancy number (N_v) of less than about 2.45 when calculated using the PHACOMP control method (6,12,13). (See Figure 3.0244.)

Embrittlement which occurs on long-time exposure at 1300 to 1600 F can be restored by re-solution heat treatment (see Figure 3.0243).

1.092 During welding, surface contamination by metallic copper which can stem from copper welding fixtures should be avoided. Copper contamination—even of a minute nature—can catalyze severe heat-affected zone cracking. This phenomenon (common to other cobalt-base alloys as well) can be best prevented by chromium electroplating of all copper jigs and fixtures (11).

Cracking is intergranular and is caused by liquid metal embrittlement by as little as 0.003 mil of copper on the alloy surface (32,62).

Do not use brazing alloys that contain copper (10).

1.093 Remove grease, graphite, and other foreign matter from all surfaces prior to heat treatment. Carburization of the alloy can reduce corrosion resistance and ductility (10).

Oxy-acetylene welding is not recommended because of the suceptibility of carbon pick-up from the acetylene flame (11).

Avoid heating in sulfur-containing atmospheres which can result in sulfur penetration and subsequent detrimental effects on mechanical properties and corrosion resistance (10).

1.094 Proper control of the temperature and time cycles when solution treating or hot-working is important. Overheating above the recommended solution treating temperature (2125 to 2175 F) can cause excessive grain growth (10). (see Section 3.015.)

The solution heat treatment is normally used for stress relieving after forming operations. During forming, avoid introducing a critical amount of strain which can produce abnormal grain growth upon subsequent annealing (See Section 4.011).

1.095 Exposure to hydrazine (N_2H_4) decomposition products at 1800 F causes embrittlement of Haynes Alloy No. 188, although the alloy may be suitable for use in this environment at lower temperatures. Hydrazine is of interest as a storable monopropellant for auxiliary power units in airborne applications and aboard the space shuttle. It decomposes into ammonia, hydrogen, and nitrogen (see Section 2.0351).

2 PHYSICAL PROPERTIES AND ENVIRONMENTAL EFFECTS

2.01 Thermal Properties

2.011 Melting Range—2375 to 2475 F (11).

2.012 Phase Changes. The alloy is subject to carbide precipitation (secondary M_6C and $M_{23}C_6$) upon elevated temperature exposure (6.11). Laves phase may also form in some heats (see Section 1.091) when exposed for long times in the range of about 1300 to 1700 F (see Figure 2.0121).

2.0121 Microconstituents occurring upon elevated temperature exposure, Figure 2.0121.

2.0122 Time-temperature-transformation diagrams.

2.013 Thermal conductivity, Figure 2.013.

2.014 Thermal expansion, Figure 2.014.

2.015 Specific heat, Figure 2.015.

2.016 Thermal diffusivity, Figure 2.016.

2.02 Other Physical Properties

2.021 Density, 0.330 lb/in.^{3}, 9.13 g/cm^3 (1,7,14).

2.022 Electrical properties.

2.0221 Electrical resistivity, 36.3 microhm-in., 92.2 microhm-cm (1,7)

2.023 Magnetic properties.

2.0231 Magnetic permeability, 1.01 at 200 oersteds (1,14).

2.024 Emittance, 0.528 at wavelengths of 0.8 micrometer at 75 F (33).

2.025 Damping capacity.

2.03 Chemical Environments

2.031 Corrosion.

2.0311 In aqueous environments over a wide range of organic and inorganic acids, it is similar to the L-605 alloy in terms of corrosion resistance.

2.0312 Corrosion rates in severe aqueous environments for Haynes Alloy No. 188, L-605, and Hastelloy B and C, Table 2.0312.

2.0313 Effect of cold work on corrosion in boiling 10 percent sulfuric acid, Table 2.0313.

2.032 Stress corrosion.

2.0321 Specimens loaded by bending to produce a maximum fiber stress equal to 80 percent F_{ty} did not show any evidence of cracking after 1000 hours of alternate immersion testing in a 3.5 percent sodium chloride solution at room temperature. The cycle consisted of immersion in the NaCl solution for 10 minutes followed by drying above the solution for 50 minutes (29).

2.033 Oxidation.

2.0331 AMS 5608 (sheet, strip, and plate) and AMS 5772 (bars, forgings, and rings) require that the thickness of metal converted to oxide plus any continuous intergranular oxidation not exceed 0.015 in./side after four 25-hr air exposures at 2000 to 2100 F (3,4).

2.0332 Haynes Alloy No. 188 has excellent oxidation resistance up to 2000 F, attributed to its high chromium content and to small additions of lanthanum. The scale which forms during high temperature air exposure consists of Cr_2O_3 and a mixed spinel, primarily $CoCr_2O_4$. Lanthanum is considered to promote adhesion of the scale. At 2100 F and above, volatile $CoWO_4$ forms and increases the rate of oxidation. In terms of total metal affected, short-term 100-hr data (Figures 2.0334 and 2.03311) indicate that Haynes Alloy No. 188 has an advantage over Hastelloy X and L-605. Longer term data to 10,000 hr, however, show similar depths of total metal affected for all three alloys (Table 2.0336). Oxidation weight changes,

which reflect surface scale and spalling, are substantially more affected by the nature of the exposure than is the depth of total metal affected. For example, burner rig exposure results in greater metal loss through surface scaling than does furnace exposure in still air, Figures 2.0337 and 2.0338 (1,11,34-37).

2.0333 Oxidation of sheet in slowly moving air, Figure 2.0333.

2.0334 Oxidation resistance in dry air (100-hr test) for Haynes Alloy No. 188 versus Hastelloy X and L-605 alloys showing continuous penetration from original thickness, Figure 2.0334.

2.035 Oxidation weight loss after intermittent exposure for 100 hr in dry air (based on descaled weight change) for Haynes Alloy No. 188 versus Hastelloy X and L-605 alloys, Table 2.035.

2.0336 Long-time oxidation behavior in still air at 1830 F, Table 2.0336.

2.0337 Oxidation weight changes during cyclic furnace and burner rig exposures at 2000 F, Figure 2.0337.

2.0338 Calculated metal losses after cyclic furnace and burner rig oxidation exposures for 100 hr at 1900 to 2100 F for Haynes Alloy No. 188, L-605, and Hastelloy X, Figure 2.0338.

2.0339 Dynamic oxidation of Haynes Alloy No. 188 after 100 hr at 1600 to 2000 F, Figure 2.0339.

2.03310 Dynamic oxidation weight change behavior of thin sheet at 2000 F, Figure 2.03310.

2.03311 Oxidation resistance under dynamic conditions of Haynes Alloy No. 188 versus other sheet alloys, Figure 2.03311.

2.03312 Silicon additions adversely affect the oxidation behavior of Haynes Alloy No. 188 at 1830 F while yttrium additions effect a minor improvement, as shown in Figure 2.03313. The scales formed remained protective but the parabolic oxidation rate increased monotonically with increasing silicon content. An exception was the modified alloy containing 0.2Y + 7.5 Si, which oxidized more slowly than that containing 0.2Y + 5Si. The outer layer of oxide scale was very susceptible to spalling in the modified alloys containing 5 or 7.5Si. The adverse effect of silicon is attributed to an increase in ionic transport rates through the p-type semiconducting Cr_2O_3 scale. The high silicon containing alloys were also very brittle (38).

2.03313 Effects of silicon and yttrium on oxidation rate of Haynes Alloy No. 188 at 1830 F, Figure 2.03313.

2.03314 Oxidation resistance under some of the environmental conditions that might be encountered by a space shuttle thermal protection system. Sheet specimens of 0.015-inch thickness which were cyclically, self-resistance-heated to 2200 F in a still air environment at a pressure of 0.2 psi (10 torr) for 100 30-min cycles (50-hr exposure at temperature) showed a weight loss of 0.4 mg/cm² and a metal loss of 0.00035 in. per side. Test cycle used was 30 min at 2200 F followed by a 6 min cooling cycle, although the specimen cooled to room temperature in a few seconds. Test samples were not descaled after exposure and prior to weighing (26,27).

2.03315 Oxidation behavior at 1800 F and air pressure of 8 torr, Figure 2.03315.

2.03316 Oxidation resistance in an arc jet simulating space shuttle entry conditions. In an arc-heated, supersonic test stream with a Mach number of approximately 6, temperature of 2020 F, and surface pressure of 0.15 psi (7.6 torr), specimens of 0.017-in.-thick sheet showed a weight loss of 7.5 mg/cm² and a total metal thickness loss of 0.0015 in. after 50 30-min cycles (25 hr exposure at temperature). A typical test cycle consisted of inserting the specimens into the arc-heated stream for 30 min and then removing them from the stream to cool (28).

	Co
Low	C
22	Cr
22	Ni
14	W
.08	La

Haynes Alloy No. 188

In a separate study (33), specimens of Haynes Alloy No. 188 along with TD-NiCr, DS-NiCr, TD-NiCrAl, and TD-NiCrAlY were heated for 25 10-min cycles in a plasma arc tunnel at an air velocity of Mach 4.6. Surface pressure at the specimens was 0.2 psi (10 torr). Weight changes for the 3x3-inch specimens were greater for Haynes Alloy No. 188 at 200 F (−91 mg) than for the TD and DS materials at 2200 F (−12 to +51 mg). These weight changes are relative (not specific) since the edges were gripped in water-cooled holders.

2.03317 Tests on a shingled, corrugated thermal protection system model constructed of Haynes Alloy No. 188 indicated good thermal protection to the underlying primary structure during radiant heating to 1800 F at Mach 4.5 and 6.7 at a dynamic pressure of 9 psi (39).

2.034 Hot corrosion.

2.0341 Haynes Alloy No. 188 has good resistance to hot corrosion. The hot corrosion behavior of Haynes Alloy No. 188 is compared with those of S-57 (Co-25Cr-10Ni-5Ta-3Al-0.5Y, developed specifically for hot corrosion resistance), IN-617, and TD-NiCrAl in Table 2.0342. The total metal affected-side for Haynes Alloy No. 188 is two to four times greater in the presence of sea salt than during straight cyclic oxidation (zero sea salt). The extent of attack for sea salt concentrations of 0.5 to 5 ppm is slightly greater at 1650 F than at 1830 F and increases with increasing amount of sea salt. The hot corrosion reaction is attributed to Na_2SO_4 which forms by reaction of NaCl with sulfur contaminant in the fuel. The presence of 4 ppm Na_2SO_4 in the combustion air caused slightly more hot corrosion than 5 ppm sea salt, both of which are equivalent in terms of sea salt content. This difference in attack is attributed to incomplete conversion of sea salt to Na_2SO_4 during the 2 msec residence time in the burner rig. The predominant oxide phases in the retained scale on Haynes Alloy No. 188 after oxidation and after hot corrosion were spinel (M_3O_4) and Cr_2O_3. When corroded with 5 ppm sea salt, the alloy became enriched with sulfides just beneath the scale and within the grain boundaries. At 1830 F, the retained scale was thicker than at 1650 F under all salt conditions. Internal oxidation was also observed (40).

2.0342 Hot corrosion of Haynes Alloy No. 188 and three other high temperature sheet alloys in Mach 0.3 burner rig at 1650 and 1830 F, Table 2.0342.

2.0343 Hot corrosion of Haynes Alloy No. 188 and other sheet superalloys after 200 hours at 1650 F, Figure 2.0343.

	Co
Low	C
22	Cr
22	Ni
14	W
.08	La

Haynes Alloy No. 188

2.0344 Haynes Alloy No. 188 is subject to severe corrosion by molten salt at high temperatures in the presence of oxygen. Mechanical properties are adversely affected. Molten salt corrosion is of interest for aircraft and space vehicles which may become salt-laden due to exposure to ocean spray. Room temperature tensile properties of salt-coated alloy sheet after high temperature exposure in air, argon, or Ar-1 percent O (simulating low-pressure air such as that encountered upon re-entry) are given in Table 3.02110 (41,42). Small amounts of salt, from 0.15 to 2.4 mg/cm², cause a reduction in ductility after 1400 F exposure. Exposure at 1800 F in air or Ar-1 percent O causes substantial reduction in both residual strength and ductility. Argon exposure of salt-coated specimens does not degrade subsequent tensile properties, indicating that oxygen is a necessary component of the salt corrosion reaction. Creep-rupture properties of bare and salt-coated alloy sheet at 1800 F are given in Table 3.0419 (42). The creep resistance and ductility are again reduced, substantially in air and Ar-1 percent 0 and moderately in argon. Separate studies (43) of Haynes Alloy No. 188 in molten NaCl established that the corrosion rates are highly dependent on oxygen, increasing with increasing oxygen pressure. Nonprotective scales were formed which consist of $CoWO_4$, $CoNiO_2$, $CoCr_2O_4$, and/or $NiCr_2O_4$. A thickness reduction of 3.5 mils was observed for 20-mil sheet after 24 hr exposure in molten salt at 1510 F in an air furnace. This high rate of uniform attack was accompanied by further intergranular oxide penetration to a depth of about 4 mils. Chromium loss was also observed at the grain boundaries. These observations indicate that the reduction of mechanical properties is largely due to intergranular corrosion.

2.035 Reactions with other gases.

2.0351 Exposure to hydrazine decomposition products at 1800 F causes subsurface hardening and degradation of mechanical properties through nitriding. Hardness traverses indicate internal nitridation to a depth of about 15 mils after a 1000-hr/1800 F exposure to partially dissociated ammonia (representative of hydrazine decomposition), Figure 2.0352. Tensile ductility at 1800 F is substantially reduced after 1800 F exposure. Haynes Alloy No. 188 is also brittle in bending at room temperature after a 1000-hr/1800 F exposure to ammonia. These property changes render Haynes Alloy No. 188 unattractive for applications involving exposure to nitrogen compounds such as ammonia or hydrazine at 1800 F or higher (44).

At 1450 and 1600 F, the alloy exhibits no significant decrease in tensile properties attributable to a $NH_3/N_2/H_2$ environment for exposure times of 2 hr. The low cycle fatigue life in compression at 1450 F is, however, slightly lower in 700 psi $NH_3/N_2/H_2$ than in argon, as shown in Figure 3.0512 (45). The high cycle fatigue behavior in tension at 1250 F in products of dissociated hydrazine (obtained by dissociating anhydrous ammonia) is shown in Figure 3.0513. However, conclusions cannot be drawn from these latter data since comparable data in other atmospheres are not available (46).

It may be concluded that fatigue properties of Haynes Alloy No. 188 are more significantly affected than tensile properties by exposure to hydrazine decomposition products at intermediate temperatures. The alloy may be useful in these environments for short times at temperatures up to about 1600 F.

2.0352 Cross-section hardness curves after exposure to partially dissociated ammonia at 1800 F, Figure 2.0352.

2.04 **Nuclear Environments**

3 MECHANICAL PROPERTIES

3.01 **Specified Mechanical Properties**

3.011 AMS specified mechanical properties, Table 3.011.

3.012 AMS 5608 specifies that specimens heated to 1195 to 1205 F, held at heat for 10 min before testing, and tested at 1195 to 1205 F at a strain rate of 0.003 to 0.007 in./in./min through the yield strength and a cross-head speed of 0.5 in./min above the yield strength shall have F_{tu} of 90 ksi minimum, F_{ty} of 36 ksi minimum, e (in 2 in. or 4D) of 40 percent minimum for material up to 0.020-in. nominal thickness and 50 percent minimum over 0.020-in. thickness. Direction of tensile test specimen is the same as given in (a), Table 3.011 (3).

3.013 AMS 5772 specifies that rupture time at 1697 to 1703 F shall be 23 hr minimum when an initial axial stress of 13 ksi is applied continuously to specimens from bars and flash-welded rings, and 12 ksi to specimens from forgings. The test shall be continued to rupture without change of load. Elongation after rupture shall be not less than 15 percent in 4D.

3.014 AMS 5608 specifies that rupture time at 1697 to 1703 F shall be 23 hr minimum when an initial axial stress of 11 ksi is applied continuously to specimens from material over 0.020 in. in nominal thickness and 9 ksi when thickness is 0.020 in. or less. The test shall be continued to rupture without change of load. Elongation in 2 in. or 4D after rupture shall be not less than 15 percent for material over 0.020-in. thickness and 8 percent when thickness is 0.020 in. or less.

3.015 AMS 5608 specifies that grain size shall be ASTM 4 or finer.

3.02 **Mechanical Properties at Room Temperature**

3.021 Tension—stress-strain diagrams—tension properties.

3.0211 Stress-strain diagrams. (See Figures 3.03112 and 3.03113.)

3.0212 Typical mechanical properties at room temperature for various mill products, Table 3.0212.

3.0213 Typical mechanical properties at room temperature of welded sheet, Table 3.0213.

3.0214 Effect of cold rolling at room temperature on the mechanical properties of sheet, Table 3.0214.

3.0215 Effect of cold rolling followed by aging on the mechanical properties of sheet, Figure 3.0215.

3.0216 Effect of elevated temperature exposure on the room temperature mechanical properties of sheet, Table 3.0216.

3.0217 Effect of aging on room temperature elongation of Haynes Alloy No. 188 versus Hastelloy X and L-605, Figure 3.0217.

	Co
Low	C
22	Cr
22	Ni
14	W
.08	La

Haynes Alloy No. 188

3.0218 Embrittlement occurs after 1600 F long-time exposure stressed or unstressed. Stress has no effect on the embrittlement reaction (47).

3.0219 Effect of thermal cycling at two thermal profiles (inset) on room temperature properties of exposed sheet, Figure 3.0219. [The exposure conditions were based on temperatures predicted for specific vehicle locations by the Launch and Entry Vehicles Group of Convair Division on a Convair-designed, medium hypersonic L/D lifting re-entry spacecraft during a typical re-entry trajectory. The thermal profiles were obtained by selecting several constant temperature levels that closely approximated the shape of the real temperature versus time curves (21)].

3.02110 Effects of salt on post-exposure tensile properties at room temperature, Table 3.02110.

3.022 Compression—stress-strain diagrams—compression properties.

3.0221 Stress-strain diagrams. (See Figures 3.03211 and 3.03212.)

3.023 Impact.

3.0231 Impact strength of plate at room temperature in the solution treated condition and after elevated temperature exposure, Table 3.0231.

3.0232 Effects of aging at elevated temperatures on notch-impact energy at room temperature,, Figure 3.0232.

3.0233 Aging time-temperature curves for 25, 50, and 75 percent reductions in notch-impact energy at room temperature for Haynes Alloy No. 188 and L-605, Figure 3.0233.

3.024 Bending.

3.0241 Bend ductility of aged sheet, Figure 3.0241.

3.0242 Effect of elevated temperature exposure on bend ductility of Haynes Alloy No. 188 and L-605 sheet, Figure 3.0242.

3.0243 Effect of subsequent resolution heat treatment and additional aging on bend ductility of sheet previously subjected to elevated temperature exposure, Figure 3.0243.

3.0244 Effect of average electron-vacancy number (N_v), determined from chemical composition, on bend ductility of sheet after exposure at 1600 F, Figure 3.0244.

3.025 Torsion and shear.

3.0251 Mill annealed sheet with F_{tu} = 146 ksi and F_{ty} = 73 ksi has a shear strength of 134 ksi in single shear (29).

A separate determination on mill-annealed sheet gave an ultimate shear strength at room temperature (average of 23 tests) of 126.0 ± 3.2 ksi in a single shear (48).

3.026 Bearing.

3.0261 Bearing tests conducted at room temperature in accordance with ASTM E238 gave F_{bru} as 317.3 ± 2.8 ksi (average of six tests) and F_{bry} as 140.1 ± 3.5 ksi (average of nine tests) (48).

3.027 Stress concentration.

3.0271 Notch properties.

3.0272 Fracture toughness.

3.028 Combined properties.

3.03 **Mechanical Properties at Various Temperatures**

3.031 Tension—stress-strain diagrams—tension properties.

3.0311 Stress-strain diagrams. See Figure 3.03111 for a typical curve at 1600 F. Discontinuous yielding (Portevin-LeChatelier effect) has been observed during tensile tests conducted in the range of 1200 to 1600 F (14).

3.03111 Stress-strain curve at 1600 F, Figure 3.03111.

3.03112 Typical stress-strain curves for sheet tested in the longitudinal direction at room and elevated temperatures, Figure 3.0312.

3.03113 Typical stress-strain curves for sheet tested in the transverse direction at room and elevated temperatures, Figure 3.0313.

3.0312 Effect of test temperature on tensile properties of sheet, plate, and bar, Figure 3.0312.

3.0313 Effect of test temperature on tensile properties of sheet tested in the longitudinal and transverse directions, Figure 3.0313.

3.0314 Effect of temperature on average tensile properties of thin sheet tested in the longitudinal and transverse directions, Figure 3.0314.

3.0315 Effect of test temperature on tensile properties of sheet after exposure at elevated temperatures, Figure 3.0315.

3.0316 Effect of test temperature on tensile properties of sheet after long-time exposure at 1500 F, Figure 3.0316.

3.0317 Effect of test temperature on yield strength of cold rolled sheet, Figure 3.0317.

3.0318 Effect of test temperature on the ultimate tensile strength of cold rolled sheet, Figure 3.0318.

3.0319 Effect of test temperature on the tensile elongation of cold rolled sheet, Figure 3.0319.

3.03110 Effect of test temperature on tensile properties of 30 percent cold rolled and aged sheet, Figure 3.03110.

3.03111 Tensile properties of Haynes Alloy No. 188 at 1800 F after exposure to partially dissociated ammonia at 1800 F, Figure 3.03111.

3.032 Compression—stress-strain diagrams—compression properties.

3.0321 Stress-strain diagrams.

3.03211 Typical compression stress-strain and tangent modulus curves for sheet tested in the longitudinal direction at room and elevated temperatures, Figure 3.03211.

3.03212 Typical compression stress-strain and tangent modulus curves for sheet tested in the transverse direction at room and elevated temperatures, Figure 3.03212.

3.03213 Effect of test temperature on the compressive yield strength of sheet tested in the longitudinal and transverse directions, Figure 3.03213.

3.033 Impact.

3.0331 Effect of test temperature on impact strength of plate, Table 3.0331.

3.0332 Effects of aging at elevated temperatures on notch-impact energy at 570 F, Figure 3.0332.

3.034 Bending.

3.035 Torsion and shear.

3.0351 Lap-shear strength of brazed joints, Table 3.0351.

3.036 Bearing.

3.037 Stress concentration.

3.0371 Notch properties.

3.0372 Fracture toughness.

3.038 Combined properties.

3.04 **Creep and Creep-Rupture Properties**

3.041 Creep-strain and creep-rupture curves for 100- and 1000-hr life of sheet at 1400 to 2000 F, Figure 3.041.

	Co
Low	C
22	Cr
22	Ni
14	W
.08	La

Haynes Alloy No. 188

3.042 Creep-rupture curves at 1300 to 2000 F for solution heat treated sheet, Figure 3.042.

3.043 Creep-rupture curves at 1400 to 2000 F for sheet tested in longitudinal and transverse directions, Figure 3.043.

3.044 Average creep-rupture life at 1500 to 2000 F of 20 production heats of sheet based on short-time quality control tests, Table 3.044.

3.045 Effect of sheet thickness on rupture life at 1500 and 2000 F, Figure 3.045.

3.046 Comparison of 100- and 1000-hour creep-rupture life of Haynes Alloy No. 188 sheet at 1400 to 2000 F with L-605 and Hastelloy X sheet, Figure 3.046.

3.047 Effect of stress and temperature on minimum creep rate of sheet, Figure 3.047.

3.048 Effect of stress and temperature on minimum creep rate of thin sheet, Figure 3.048.

3.049 Comparison of minimum creep rate stresses of Haynes Alloy No. 188 sheet at 1400 to 1800 F with Hastelloy X sheet, Figure 3.049.

3.0410 Stress versus 0.5 percent creep curves for sheet at 1400 to 2000 F, Figure 3.0410.

3.0411 Stress versus 1.0 percent creep curves for sheet at 1400 to 2000 F, Figure 3.0411.

3.0412 Average creep-strain curves at 1200 to 1800 F for thin sheet tested in longitudinal and transverse directions, Figure 3.0412.

3.0413 Comparison of 100- and 1000-hour 0.5 percent creep strength of Haynes Alloy No. 188 sheet at 1400 to 2000 F with Hastelloy X sheet, Figure 3.0413.

3.0414 Creep-strain and creep-rupture curves for sheet at 800 to 1600 F tested in the transverse direction, Figure 3.0414.

3.0415 Effect of grain size on creep rate of 15-mil sheet at 1700 F and 6 ksi, Table 3.0415.

3.0416 The time to reach 0.5 percent creep strain at 1600 and 1800 F increases with increasing amount of cold prestrain, as shown in Figure 3.0417. The increase in time at 1600 F for a prestrain of 15 percent is more than a factor of 10, equivalent to an increase in creep strength of 60 percent. The beneficial effects of prestraining disappear after about 1000 hours at 1600 F or 10 hours at 1800 F. The creep strength improvement is associated with dislocation pinning by $M_{23}C_6$ precipitate (59).

3.0417 Effect of prestraining at room temperature on 0.5 percent creep strain curves at 1600 and 1800 F, Figure 3.0417.

3.0418 Effect of thermal-mechanical processing on 0.5 percent creep strength of thin sheet at 1200 to 1800 F, Figure 3.0418.

3.0419 Effects of salt and test atmosphere on creep-rupture properties at 1800 F and 5.25 ksi, Table 3.0419.

3.05 **Fatigue Properties**

3.051 Low cycle fatigue data at 1700 F for Haynes Alloy No. 188, Hastelloy X, and GTA-welded Haynes Alloy No. 188, Figure 3.051.

3.052 Axial-load fatigue strength of unnotched sheet at room and elevated temperatures tested in the transverse direction, Figure 3.052.

3.053 Axial-load fatigue strength of notched sheet at room and elevated temperatures tested in the transverse direction, Figure 3.053.

3.054 Axial-load fatigue strength of unnotched thin sheet at room and elevated temperatures tested in the longitudinal direction, Figure 3.054.

3.055 Low cycle fatigue crack-growth rates are presented in Figure 3.056 and summarized in Figure 3.057. The high value of the exponent m in the empirical relation $da/dn = A\Delta K^m$ is attributed to the high work hardening rate of Haynes Alloy No. 188 and reflects good resistance to fatigue crack growth. The exponent m decreases from 6.6 at room temperature and 1110 F to 5.5 at 1600 F as a result of increasing recovery and decreasing rate of work hardening. The influence of cyclic frequency on the crack-growth rate is negligible at high frequencies but below a critical frequency the crack-growth rate increases rapidly with decreasing frequency, as shown in Figure 3.058. At the same time, the fracture path changes from transgranular to intergranular. Also shown in Figure 3.058 is a creep crack-growth line derived from creep crack measurements on specimens from the same lot of material. The creep crack-growth curve serves as a lower limit for fatigue crack-growth rates. Crack-growth rates in the transition region between pure fatigue and pure creep are affected by oxidation. The transition region is relatively narrow here because of the good oxidation resistance of Haynes Alloy No. 188. Of further interest are the crack-growth rates expressed in time units rather than cycles, as shown in Figure 3.059. The crack-growth rates are seen to increase with increasing cyclic frequency. For example, the rates at a frequency of 10 cycles/sec are more than two magnitudes greater than those for steady creep under (static) loading (49,63).

3.056 Fatigue crack-growth rates at 1110 to 1600 F, Figure 3.056 [(a) 1110 F, (b) 1400 F, and (c) 1600 F].

3.057 Fatigue crack-growth rates at a frequency of 10 cps at room temperature and elevated temperatures, Figure 3.057.

3.058 Frequency and temperature dependence of fatigue and creep crack-growth rates, Figure 3.058.

3.059 Crack growth per second at 1110 F under steady state creep and under cyclic loading at various frequencies, Figure 3.059.

3.0510 The low cycle fatigue life of Haynes Alloy No. 188 is moderately degraded in 5000 psi hydrogen at both room temperature and 1250 F as compared to testing in 5000 psi helium, as shown in Figure 3.0511. Degradation of Haynes Alloy No. 188 is more severe than the iron-base alloys A-286 and stainless steel Type 347 but less severe than the nickel-base alloys Inconel Alloy 718, Inconel Alloy 625, and Waspaloy (46,50).

3.0511 Effects of high pressure hydrogen on low cycle fatigue life of Haynes Alloy No. 188, Figure 3.0511 [(a) room temperature and (b) 1250 F].

3.0512 Effects of hydrazine decomposition products on low cycle compressive fatigue at 1450 F, Figure 3.0512.

3.0513 High cycle fatigue strength of Haynes Alloy No. 188 at 1250 F in hydrazine, Figure 3.0513.

3.06 **Elastic Properties**

3.061 Poisson's Ratio, Figure 3.061.

3.062 Modulus of elasticity, Figure 3.062.

3.063 Modulus of rigidity.
3.064 Tangent modulus (see Figures 3.03211 and 3.03212).
3.065 Secant modulus.

4 FABRICATION

4.01 Forming

4.011 General. Cold working is the preferred method for bending, deep drawing, and spinning the alloy into various shapes. It has excellent ductility, but tends to work harden to greater extent than the austenitic stainless steels. Consequently, more intermediate stages of deep drawing or cold forming may be required to produce the final part. Annealing at 2150 F followed by rapid cooling will restore the original ductility. Lower intermediate annealing temperatures will produce a fine-grained structure with less formability and a higher tensile strength than the original material. Most parts will require a solution anneal at 2150 F after final cold working.

Strain introduced during any cold working operation should exceed at least 12 percent cold reduction. Critical strain (cold working to the extent of about 2 to 12 percent) produces abnormal grain growth upon subsequent annealing and should be avoided.

Care should be taken to remove all lubricants or die material before annealing, since many of these preparations will affect the characteristics of the alloy (see Sections 1.093 and 1.097). It is also desirable to remove scale from the annealed part prior to the next forming operation, either by pickling or suitable mechanical means (10,11,22).

4.012 Press forming or drawing the alloy generally requires about twice as many intermediate anneals as for austenitic stainless steels. With proper lubrication and die design, some of the simpler operations can be performed without an intermediate anneal (10).

4.013 Spinning operations usually work harden the alloy somewhat more than press forming. Annealing betwen spinning operations is, therefore, recommended, although fairly severe reductions are possible in light gages without intermediate anneals (10).

4.014 Drop-hammering operations to form Haynes Alloy No. 188 sheet utilize the same techniques used for stainless steel. Annealing is essential if the depth of draw is severe (10).

4.015 Punching is usually performed cold. Perforations should be limited to a minimum diameter of twice the gage thickness. The center-to-center dimension should be about three to four times the hole diameters (10).

4.016 Erichsen cup depth test results at room temperature range from 0.56 in. for 0.078-in.-thick sheet to 0.46 in. for 0.020-in.-thick sheet in the 2150 F solution treated condition (1,11).

4.017 Bend properties. (See Section 3.0243.)

4.018 The tensile strain hardening exponent of the alloy varies from 0.51 at room temperature to 0.32 at 1350 F, then stabilizes at a value of approximately 0.11 from 1450 to 1600 F at a strain rate of 0.005 in./in./min (11,14).

4.019 Forging. Initial forging temperature is 2150 to 2175 F maximum and finishing temperature is 1800 F minimum. On initial forging of ingots, avoid making radical changes in cross-sectional shape, such as going directly from a square to a round. After the cast structure has been broken up, moderately heavy reductions of 25 to 40 percent are beneficial in maintaining as much internal heat as possible, thereby minimizing the number of reheatings and grain coarsening (10).

	Co
Low	C
22	Cr
22	Ni
14	W
.08	La

Haynes Alloy No. 188

4.0110 The effects of thermal-mechanical processing (TMP) on the creep properties of Haynes Alloy No. 188 have been evaluated by Klarstrom (36). Significant improvements in the low strain creep strength were obtained in thin sheet by fabricating to a strong crystallized texture. The TMP schedule considered to give optimum strengthening consisted of 80 percent final cold work followed by a 10-min anneal at 2250 F. The major components of the texture resulting from this TMP schedule, with respect to the plane of the sheet and the rolling direction, were identified as (110) [110] and (112) [110]. The 0.5 percent creep strength of textured sheet is up to 70 percent greater than that of baseline untextured (production) sheet, as shown in Figure 3.0418. Grain size also affects creep behavior, although not as much as TMP. Relative to baseline sheet with a grain size of ASTM 6 to 6½, experimental sheet processed to a coarser grain size of ASTM 2 to 4 exhibited slightly greater times to 0.5 and 1.0 percent creep strain, as shown in Table 3.0415, and also an increase in the total amount of primary creep strain. Fine-grained sheet with a grain size of ASTM 7 to 8 is weaker in creep than coarser grained material. The creep strength is related directly to grain size but not to sheet thickness per se (36), in contrast to earlier observations summarized in Figure 3.045.

4.02 Machining and Grinding

4.021 Machining. In general, Haynes Alloy No. 188 has the same machinability characteristics as L-605 alloy. Effective machining requires the employment of proper tools and feed rates. Relatively short tool lives, however, may be expected. Due to the work-hardening nature of cobalt-base alloys, intermittent cuts should be avoided whenever possible. In general, high speed tools are applicable for most tapping, reaming, drilling, and milling operations. Carbide tools may be used for certain roughing operations provided that rigid set-ups are available.

4.022 Specific and detailed data on cutting tool materials, tool design, feed and speed rates, and lubricants for turning, facing, boring, drilling, milling, reaming, and tapping are listed in Reference 10, pp 14–17, and should be consulted before undertaking critical machining operations.

4.023 Grinding operations should be performed with aluminum oxide wheels. There is little danger of heat checking this alloy, but it can be damaged by poor grinding practice (22).

4.024 Specific and detailed data on grinding wheel description and specifications (by manufacturers' listing) for type of work and recommended lubricants are given for rough, cylinder, surface, internal, and thread grinding and for internal honing in Reference 10, p 18.

4.03 Joining

4.031 General. This alloy is amenable to joining using several conventional fusion welding processes, such

	Co
Low	C
22	Cr
22	Ni
14	W
.08	La

Haynes Alloy No. 188

as gas-tungsten arc, gas-metal arc, and electron-beam welding. Oxy-acetylene welding is not recommended because of the susceptibility of carbon pick-up from the acetylene flame. Gas-tungsten arc (GTA) welding generally produces the most satisfactory results. Because this is a solid-solution strengthened alloy, microstructural changes, due to elevated temperature cycles associated with the welding arc, are held to a minimum. Furthermore, no allotropic phase transformations are encountered in the heat-affected zone (11,12).

4.032 Good joining practices produce sound welds. Joint preparations and cleaning prior to welding are most important. Preheat is not required. Weld interpass temperatures should be under 200 F, and excessive weld heat input should be avoided.

4.033 The alloy has a relatively low heat-affected-zone (HAZ) hot-cracking susceptibility. Its HAZ characteristics are similar to Hastelloy X (a nickel-base alloy) and exhibit an improvement in weldability over L-605 (a cobalt-base alloy) (11).

4.034 Hot-zone cracking likelihood is greater if welding is done in the cold-worked condition. Any fusion welding of cold-formed parts should be preceded by a solution annealing treatment to minimize possibilities of hot cracking in the heat-affected zone (11,22).

4.035 Thin sheet is more susceptible than thick sheet to hot cracking in the heat-affected zone after gas tungsten arc welding. The extent of cracking is related to the ratio of sheet thickness to grain diameter, as shown in Figure 4.036. Hot cracking is most severe when the thickness-to-grain diameter ratio decreases to a value of 4 or less. This increased hot crack sensitivity in material with low thickness-to-grain diameter ratios apparently reflects greater ease of intergranular propagation in the heat-affected zone of cracks originating at resolidified grain boundries. Any forming operation which requires cold working and subsequent annealing prior to a fusion joining operation should be conducted so that the resulting thickness-to-grain diameter ratio will be greater than 4 (51).

4.036 Effect of sheet thickness-to-grain-diameter ratio on hot crack sensitivity of GTA-welded thin gage alloy from five heats, Figure 4.036.

4.037 Excessive restraint during welding and physical contamination by metallic copper from welding fixtures (see Section 1.097) can cause heat-affected-zone cracking and should be avoided (11,22).

4.038 Specific welding procedures and parameters for GTA, GMA, spot- and seam-welding are given in Reference 10, pp 2-9, and for electron-beam and resistance welding in Reference 16, pp 13-18.

4.039 Effect of test temperature on tensile properties of GTA-welded sheet, Figure 4.039.

4.0310 Rupture life of GTA-welded sheet, Table 4.0310.

4.0311 Brazing. The alloy can be readily joined by brazing, provided that all joining surfaces are free of all contaminants. Cleaning can be done by etching, solvent-scrubbing, degreasing, or mechanical blasting. A wide variety of brazing alloys can be used, depending upon service temperature conditions; however, brazing alloys high in copper or silver content are not recommended. Nickel-base or cobalt-base brazing alloys are recommended for most elevated-temperature applications. Brazing should be performed in a furnace under controlled-atmosphere conditions, such as argon, hydrogen, or vacuum (10,11,22).

4.0312 Diffusion bonding. Under proper conditions, parts can be successfully joined together by this technique. Complete removal of surface oxide and all contaminants is necessary followed by processing in hard vacuum environments. Temperatures approaching 2150 F are generally sufficient to obtain a metallurgical bond. For more critical applications requiring exceptional joint quality, a suitable interlayer material is generally recommended. Joint shear strengths approaching 75 percent of the tensile stress are attainable. Because the alloy has outstanding high-temperature stability, the long-time elevated-temperature thermal cycle associated with the diffusion bonding process is not harmful to the mechanical properties of the base material (11,22).

4.04 **Surface Treatment**

4.041 Cleaning. The alloy is relatively inert to cold acid pickling solutions. After heat treatment, the oxide film is more adherent than that associiated with stainless steels. Molten caustic baths followed by acid pickling have been found to be most effective in final cleaning operations. Descaling is performed at 800 to 1000 F in commercial molten salts based on sodium hydroxide with various proprietary catalytic and oxidizing agents. Subsequent acid pickling solutions depend upon thee caustic descaling medium used. Sulfuric-hydrochloric, permanganate, and nitric-hydrofluoric acid baths or combinations thereof are generally employed (22).

4.042 Specific recommendations on the composition and usage of molten caustic baths and acid pickling solutions are given in Reference 10, p 19.

REFERENCES

1 Haynes Alloy No. 188, Stellite Division, Cabot Corporation, Product Bulletin No. F-30, 361A.

2 U.S. Patent No. 3,418,111.

3 AMS 5608A sheet, strip, and plate (October 15, 1979).

4 AMS 5772A bars, forgings, and rings (July 15, 1980).

5 AMS 5801A welding wire (July 16, 1979).

6 Herchenroeder, R. B., "Aging Characteristics of Haynes Developmental Alloy No. 188", Union Carbide Corporation, Technology Department, R&D Report No. 7513 (August 1, 1968).

7 "Comparative Properties of Haynes High-Temperature Alloys", Stellite Division, Cabot Corporation, Product Bulletin No. F-30, 134D.

8 Herchenroeder, R. B. and Ebihara, W. T., "In-Process Metallurgy of Wrought Cobalt-Base Alloys", Union Carbide Corporation, Kokomo Laboratory Report (October 16, 1968).

9 Ibid, *ASM Metals Engineering Quarterly*, Vol. 9, No. 2 (May 1969).

10 Haynes Alloy No. 188 Fabrication Guide, Stellite Division, Cabot Corporation (1970).

11 Herchenroeder, R. B., Matthews, S. J., Tackett, J. W., and Wlodek, S. T., "Haynes Alloy No. 188," Report No. 8024, Stellite Division, Cabot Corporation, (November 5, 1971).

12 Boesch, W. J. and Slaney, J. S., "Preventing Sigma Phase Embrittlement in Nickel-Base Alloys", *Metal Progress*, Vol. 86, No. 1 (July 1964), pp 109–111.

13 Woodyatt, L. R., Sims,, C. T., and Beattie, H. J., Jr., "Prediction of Sigma-Type Phase Occurrence from Compositions in Austenitic Superalloys", *AIME Transactions*, Vol. 236 (April 1966), pp 519–527.

14 Ebihara, W. T. and Herchenroeder, R. B., "Mechanical and Physical Properties of Haynes Developmental Alloy No. 188", Report No. 7626, Kokomo Laboratory, Union Carbide Corporation (July 16, 1969).

15 Taylor, T. A. and Tucker, R. C., Jr., "Oxidation of a Cobalt-Base Superalloy", *Proceedings of Second Annual Sccanning Electron Microscope Symposium*, Chicago, Illinois (April 1969).

16 Wilson, J. L., "Data Summary of the Welding of Haynes Alloy No. 188 Sheet", Report No. 7606, Stellite Division, Cabot Corporation (June 24, 1969).

17 Personal communication with E. F. Bradley, Deputy Manager, Materials Engineering and Research, Pratt & Whitney Aircraft, E. Hartford, Connecticut (October 25, 1971).

18 Herchenroeder, R. B., "Properties of Cold Worked Haynes Alloy No. 188", Report No. 7846, Stellite Division, Cabot Corporation (November 9, 1970).

19 Tackett, J. W., "The Creep-Rupture Properties of Haynes Alloy No. 188", Report No. 8020, Stellite Division, Cabot Corporation (November 4, 1971).

20 Personal communication with L. P. Jahnke, Manager, Materials & Process Technology Laboratories, General Electric Company, Cincinnati, Ohio (October 4, 1971).

21 Kerr, J., R., "Evaluation of Nickel and Cobalt-Base Superalloys and Silicide-Coated Columbium Alloys for Use in Radiative Thermal Protection Systems" Report No. GDC-ERR-1345, Structures and Materials, Convair Division, General Dynamics Corporation (December 1968).

22 Herchenroeder, R. B., Matthews, S. J., Tackett, J. W., and Wlodek, S. T., "A Versatile High-Temperature Alloy", *Metal Progress*, Vol. 101, No. 103 (March 1972), pp 60–64.

23 Simmons, W. F. and Wagner, H. J., "Current and Future Usage of Materials in Aircraft Gas Turbine Engines", DMIC Memorandum 245 (February 1, 1970).

24 Simmons, W. F., "Description and Engineering Characteristics of Eleven New High-Temperature Alloys", DMIC Memorandum 255, Battelle Columbus Division (June 1971).

25 "Haynes Alloy No. 188 Stress-Rupture Properties", Stellite Division, Cabot Corporation (April 22, 1970).

26 Korb, L. J., "Heat Shield Materials Key to Space Shuttle", *Metal Progress*, Vol. 101, No. 104 (April 1972), pp 83–92.

27 Sanders, W. A. and Barrett, C. A., "Oxidation Screening at 1204 C (2200 F) of Candidate Alloys for the Space Shuttle Thermal Protection System", NASA Technical Memorandum TM X-67864, Lewis Research Center, Cleveland, Ohio (October 1971).

28 Centolanzi, F. J., Probst, H. B., Lowell, C. E. and Zimmerman, N. B., "Arc Jet Tests of Metallic TPS Materials", NASA Technical Memorandum TM X-62092, Ames & Lewis Research Center (October 1971).

29 Deel, O. L. and Mindlin, H., "Engineering Data on New Aerospace Structural Materials", Technical Report AFML-TR-71-249, Battelle Columbus Laboratories, Air Force Materials Lab Contract No. F33615-70-C-1070 (December 1971).

30 Obrzut, J. J., "Substitute Materials: Our Answer to OMEC-Type Crises", *Iron Age*, Vol. 225, No. 22 (August 2, 1982), pp 43–45.

31 Coutsouradis, D. and Habraken, L., "Metallurgical Applications of Cobalt: A Critical Overview", *Journal of Metals*, Vol. 35, No. 1 (January 1983), pp 40–47.

32 Savage, W. F., Nippes, E. F., and Mushala, M. C., "Liquid-Metal Embrittlement of the Heat-Affected Zone by Copper Contamination", *Welding Journal*, Vol. 57, No. 8 (August 1978), pp 237-s-245-s.

33 Land, D. W., "Superalloy Material Tests in a Plasma Arc Tunnel", McDonnell Douglas Corp., presented at the Sixth Space Simulation Symposium, New York City (May 1–3, 1972).

34 Angerman, C. L., "Long-Term Oxidation of Superalloys", *Oxidation of Metals*, Vol. 5, No. 2 (November 1972), pp 149–67.

35 Barrett, C. A., Johnston, J. R., and Sanders, W. A., "Static and Dynamic Cyclic Oxidation of 12 Nickel-, Cobalt-, and Iron-Base High-Temperature Alloys", *Oxidation of Metals*, Vol. 12, No. 4 (August 1978), pp 343–77.

36 Klarstrom, D. L., "Thermomechanical Processing of Haynes Alloy No. 188 Sheet to Improve Creep Strength", Cabot Corporation, Kokomo, Indiana, NASA CR-3013 (August 1978).

37 Simmons, J. J., and Wlodek, S. T., "Dynamic Oxidation Data for High Performance Sheet Alloys", Cabot Corporation, Kokomo, Indiana, Research and Development Report (May 17, 1974).

38 Dries, G. A., "Hot Corrosion and Oxidation Studies of Cobalt Based Superalloys at 1000 C", Pennsylvania State University, University Park Appllied Research Laboratory, ARL/PSU/TM-79-177 (October 9, 1979).

39 Avery, D. E., "Performance of a Haynes 188 Metallic Standoff Thermal Protection System at Mach 7", NASA Langley Research Center, Hampton, Virginia, NASA TP-1802 (April 1981).

40 Santoro, G. J., "Hot Corrosion of Four Superalloys: HA-188, S-57, IN-617 and TD-NiCrAl", *Oxidation of Metals*, Vol. 13, No. 5 (October 1979), pp 405–435.

41 Nelson, E. E., "The Effect of Hot Salt on the Mechanical Properties of Several Superalloys", NASA Marshall Space Flight Center, Huntsville, Alabama, NASA TM X-64701 (October 19, 1972).

42 Paton, N. E., Robertson, W. M., and Mansfield, F., "High Temperature Behavior of Superalloys Exposed to Sodium Chloride: I. Mechanical Properties", *Metallurgical Transactions*, Vol. 4, No. 1 (January 1973), pp 317–320.

43 Mansfeld, F., Paton, N. E., and Robertson, W. M., "The High Temperature Behavior of Superalloys Exposed to Sodium Chloride: II. Corrosion",

	Co
Low	C
22	Cr
22	Ni
14	W
.08	La

Haynes Alloy No. 188

	Co
Low	C
22	Cr
22	Ni
14	W
.08	La

Haynes Alloy No. 188

Metallurgical Transactions, Vol. 4, No. 1 (January 1973), pp 321-327.

44 Marcy R. D., "Material Evaluation Program, High Temperature Nitriding Environment", Rockwell International Corporation, Canoga Park, California, NASA CR-144382 (October 1973).

45 Chandler, W. T., "The Effect of Hydrazine Decomposition Products on the Mechanical Properties of High-Temperature Alloys", Rocketdyne Division, Rockwell International Corporation, Canoga Park, California, AFML TR-77-95 (March 15, 1978).

46 Harris, J. A. and Van Wanderham, M. C., "Properties of Materials in High Pressure Hydrogen at Cryogenic, Room, and Elevated Temperatures", Pratt and Whitney Aircraft, West Palm Beach, Florida, NASA CR-124394 (July 31, 1973).,

47 Royster, D. M. and Lisagore, W. B., "Effect of High-Temperature Creep and Oxidation on Residual Room-Temperature Properties for Several Thin-Sheet Superalloys", NASA Langley Research Center, Hampton, Virginia, NASA TN D-6893 (November 1972).

48 Ruff, P. E., and Smith, S. H., "Development of MIL-HDBK-5 Design Allowable Properties and Fatigue-Crack Propagation Data for Several Aerospace Materials", Battelle Columbus Division, Columbus, Ohio, AFML TR-77-162 (October 1977).

49 Ohmura, T., Pelloux, R. M., and Grant, N. J., "High Temperature Fatigue Crack Growth in a Cobalt Base Superalloy", *Engineering Fracture Mechanics*, Vol. 53, No. 4 (December 1973), pp 909-922.

50 Van Wanderham, M. C. and Harris, J. A., Jr., "Low Cycle Fatigue of Metals in High Pressure Gaseous Hydrogen at Cryogenic, Ambient, and Elevated Temperatures", Pratt and Whitney Aircraft, presented at 1971 WESTEC Conference, Los Angeles, California (March 8-11, 1971).

51 Matthews, S. J., "Weldability Studies on High Performance Alloys in Thin Sheet Form", *Welding Journal*, Vol. 54, No. 9 (September 1975) pp 281-S-287-S.

52 Uhlig, H. H. and Asphahani, A. I., "Corrosion Behavior of Cobalt Base Alloys in Aqueous Media", *Materials Performance*, Vol. 18, No. 11 (November 1979), pp 9-20.

53 Simmons, J. J. and Wlodek, S. T., "Hot Corrosion Data for High Performance Sheet Alloys", Cabot Corporation, Kokomo, Indiana, Research and Development Report (May 17, 1970).

54 McCoy, H. E. and Bourgette, D. T., "Influence of Aging on the Impact Properties of Hastelloy N, Haynes Alloy No. 25 and Haynes Alloy No. 188", Union Carbide Corporation, Oak Ridge, Tennessee, ORNL-TM-4380 (December 1973).

55 Hammond, J. P., "Effect of Long-Term Aging at 815 C on the Tensile Properties and Microstructural Stability of Four Cobalt- and Nickel-Base Superalloys", Union Carbide Corporation, Oak Ridge, Tennessee, ORNL-5174 (August 1976).

56 Beuyukian, C. S., "Brazing of Refractory, Superalloy and Composite Materials for Space Shuttle Applications", *Welding Journal*, Vol. 50, No. 7 (July 1971), pp 491-494.

57 Stevens, E. G., "Haynes 188/Nicrobraze 30 Braze Joint and Haynes 188 Tensile Tests—IR and D Space Shuttle", Rockwell International Corporation, Downey, California, LR-7910-4028 (October 1970).

58 Klarstrom, D. L., "Thermomechanical Processing of Haynes Alloy No. 188 Sheet to Improve Creep Strength", Cabot Corporation, Kokomo, Indiana, Proceedings of the Fourth International Symposium on Superalloys, Superalloys 1980, Champion, Pennsylvania (September 21-25, 1980), pp 131-140.

59 Young, C. T., Sommers, B. R., and Lytton, J. L., "Correlation of Creep Rate with Microstructural Changes During High Temperature Creep", Virginia Polytechnic Institute and State University, Blacksburg, Virginia, NASA CR-145220 (February 1977).

60 Rutkosky, F. A., "Evaluation of Candidate Heat Shield Materials for Shuttle Vehicle", Rockwell International Corporation, Downey, California, Laboratory and Test Report (September 1970).

61 Herchenroeder, R. B., Matthews, S. J., Tackett, J. W., and Wlodek, S. T., "A Versatile High-Temperature Alloy", *Metal Progress*, Vol. 101, No. 3 (March 1972), pp 60-64.

62 Matthews, S. J. Maddock, M. O., and Savage, W. F., "How Copper Surface Contamination Affects Weldability of Cobalt Superalloys", *Welding Journal*, Vol. 51, No. 5 (May 1972), pp 326-328.

63 Jablonski, D. A., Carisella, J. V., and Pelloux, R. M., "Fatigue Crack Propagation at Elevated Temperatures in Solid Solution Strengthened Superalloys", *Metallurgical Transactions*, Vol. 8A, No. 12 (December 1977), pp 1893-1900.

Haynes Alloy No. 188		
	Percent	
Element	Minimum	Maximum
Carbon	0.05	0.015
Manganese	—	1.25
Silicon	0.20	0.50
Phosphorus	—	0.020
Sulfur	—	0.015
Chromium	20.00	24.00
Nickel	20.00	24.00
Tungsten	13.00	16.00
Lanthanum	0.02	0.12
Boron	—	0.015
Iron	—	3.00
Cobalt	Remainder	

TABLE 1.04. COMPOSITION (3,4,5)

Haynes Alloy No. 188	
Condition	Structure
Solution annealed	FCC matrix, primary M_6C, La-rich compound (La_xM_y) associated with M_6C
Aged at 1800 F	FCC matrix, primary M_6C, La_xM_y, secondary M_6C
Aged at 1600 F	FCC matrix, primary M_6C, La_xM_y, secondary M_6C, $M_{23}C_6$
Aged at 1400 F	FCC matrix, primary M_6C, La_xM_y, secondary $M_{23}C_6$
Aged at 1200 F and lower	Annealed constituents

Samples aged 200 and 500 hr at temperature

TABLE 1.054. EFFECT OF SOLUTION TREATMENT AND AGING ON MICROSTRUCTURE AND MICROCONSTITUENTS (1,6)

	Co
Low	C
22	Cr
22	Ni
14	W
.08	La

Haynes Alloy No. 188

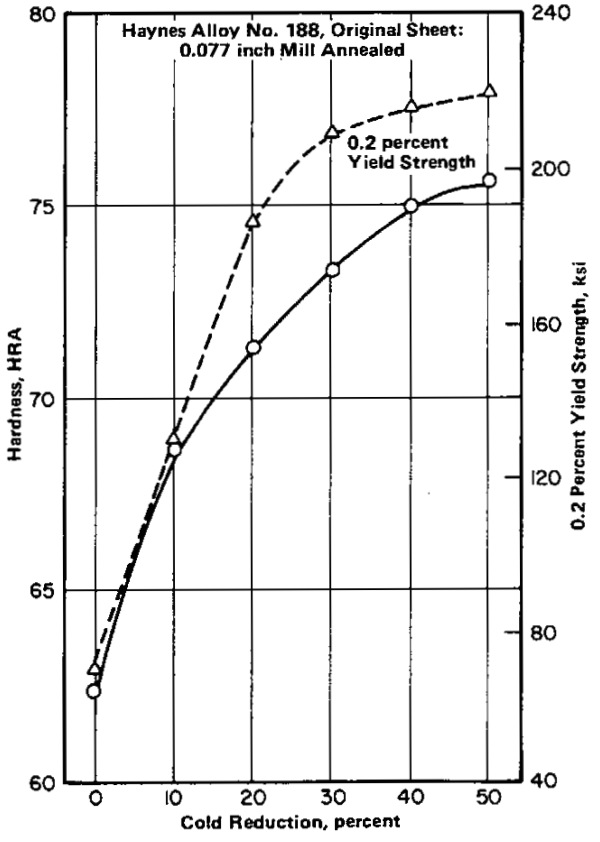

FIGURE 1.063. EFFECT OF COLD ROLLING ON THE HARDNESS AND YIELD STRENGTH OF SHEET (8,9)

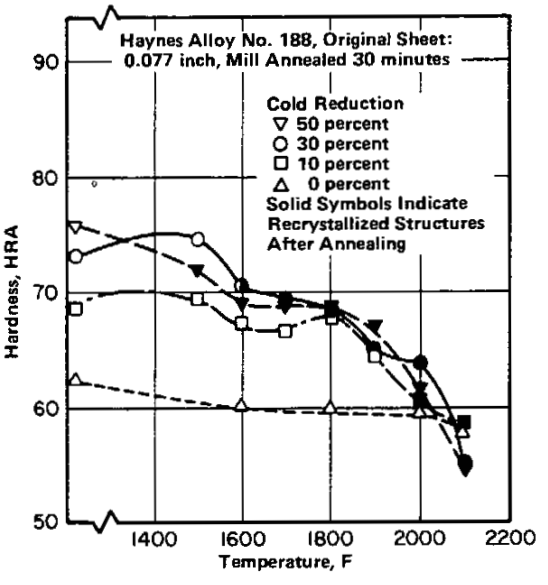

FIGURE 1.064. HARDNESS RECOVERY CHARACTERISTICS FOR COLD ROLLED SHEET UPON ANNEALING (8,9)

	Co
Low	C
22	Cr
22	Ni
14	W
.08	La

Haynes Alloy No. 188

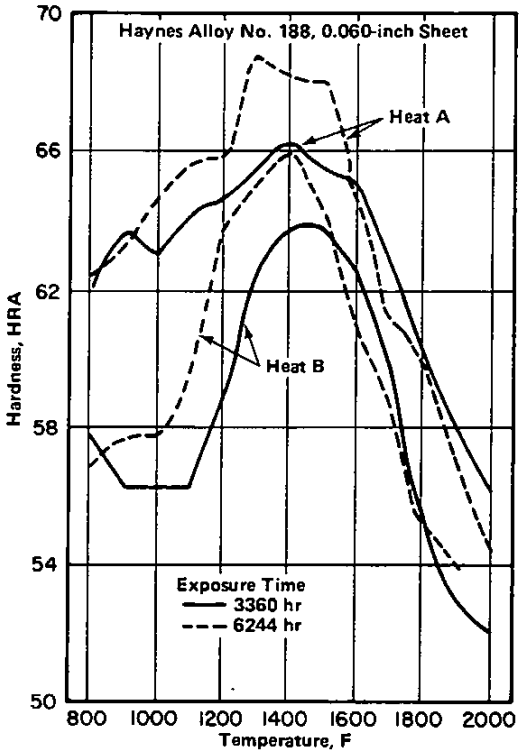

FIGURE 1.066. EFFECT OF ELEVATED TEMPERATURE EXPOSURE ON HARDNESS OF TWO HEATS (6)

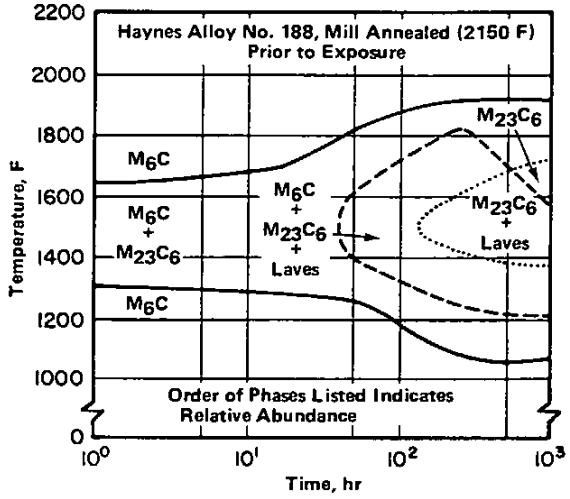

FIGURE 2.0121. MICROCONSTITUENTS OCCURRING UPON ELEVATED TEMPERATURE EXPOSURE (11)

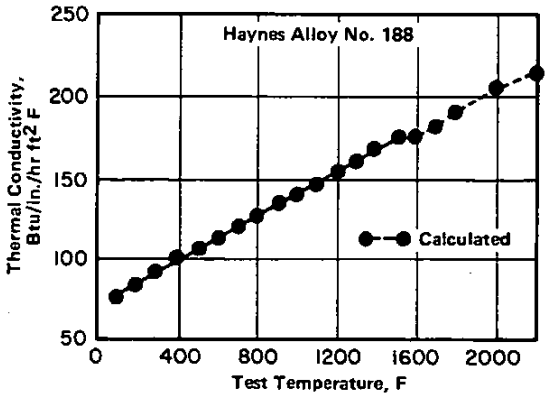

FIGURE 2.013. THERMAL CONDUCTIVITY (1,7)

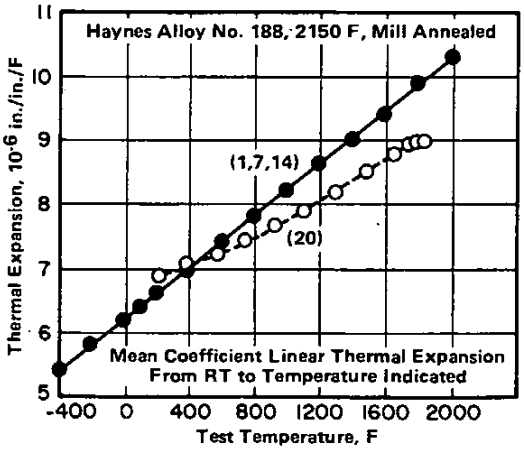

FIGURE 2.014. THERMAL EXPANSION (1,7,14,20)

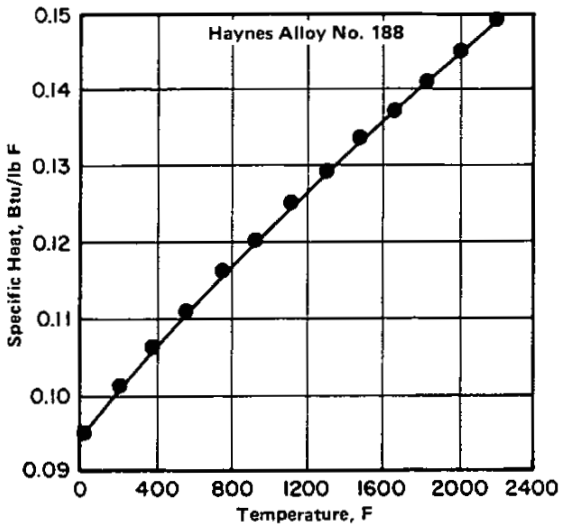

FIGURE 2.015. SPECIFIC HEAT (1,14)

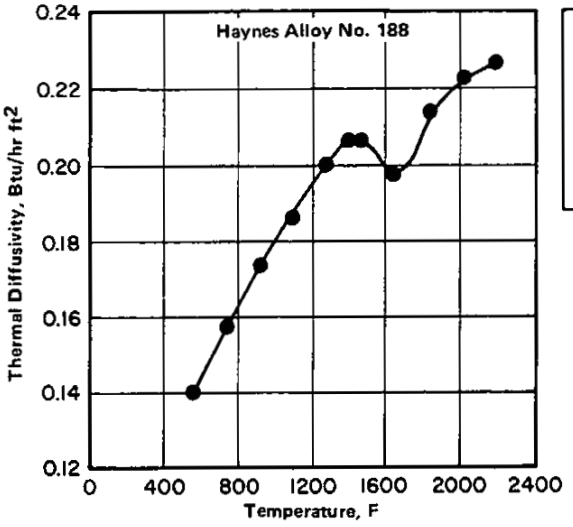

	Co
Low	C
22	Cr
22	Ni
14	W
.08	La

Haynes Alloy No. 188

FIGURE 2.016. THERMAL DIFFUSIVITY (14)

Haynes Alloy No. 188						
Medium	Concentration, weight percent	Temperature	Corrosion Rate, mils/year			
			Haynes 188	L-605	Hastelloy C	Hastelloy B
Acetic Acid	10	Boiling	—	0.1	—	—
	99	Boiling	Nil	Nil	0.1	0.2
Chromic Acid	10	Boiling	54	—	17	550
Hydrochloric Acid	10	Room	21	0.2	2	2
	5	Boiling	—	>1000	—	—
	10	Boiling	>1000	>1000	—	—
Nitric Acid	10	Boiling	0.6	0.8	—	—
	65	Boiling	22	53	820	>1000
Nitric Plus Hydrofluoric Acid	15+ 8 (vol)	150 F	30	—	—	>1000
Phosphoric Acid	10	Boiling	—	2	—	—
	55	Boiling	8	4	—	—
	85	Boiling	529	144	—	—
Sulfuric Acid	10 (vol)	Boiling	43	140	—	—
	96 (vol)	Boiling	—	76	—	—
Sulfuric Acid plus Ferric Sulfate	50 (vol) + 4.2	Boiling	18	26	—	—
Ferric Chloride plus Sodium Chloride	5+ 10	Room	Nil	—	Nil	>1000

TABLE 2.0312. CORROSION RATES IN SEVERE AQUEOUS ENVIRONMENTS FOR HAYNES ALLOY NO. 188, L-605, AND HASTELLOY B AND C (11,52)

	Co
Low	C
22	Cr
22	Ni
14	W
.08	La

Haynes Alloy No. 188

Haynes Alloy No. 188	
Cold Reduction, percent	Corrosion Rate, mils/year
0	43
10	53
30	137
50	157

TABLE 2.0313. EFFECT OF COLD WORK ON CORROSION IN BOILING 10 PERCENT SULFURIC ACID (52)

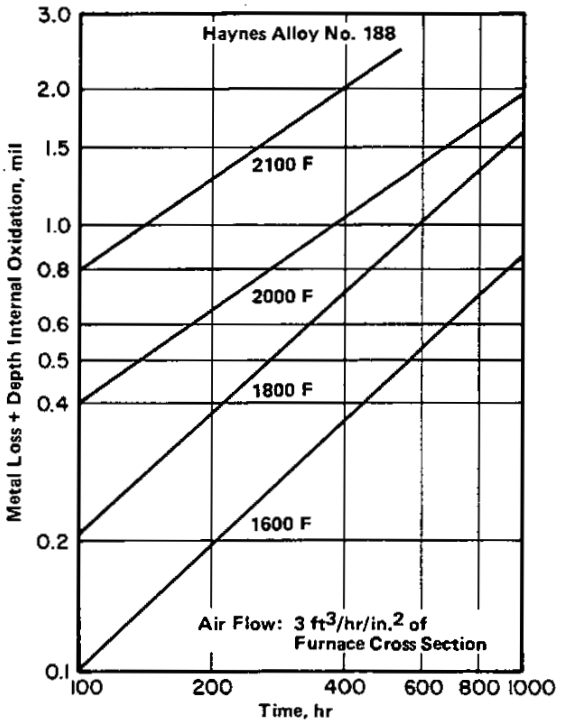

FIGURE 2.0333. OXIDATION OF SHEET IN SLOWLY MOVING AIR (11)

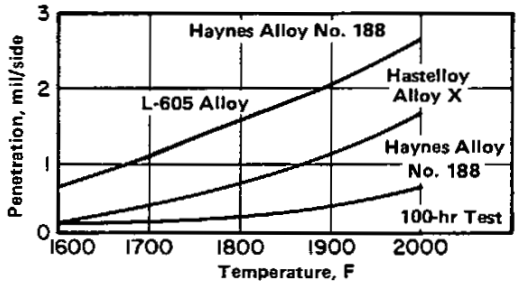

FIGURE 2.0334. OXIDATION RESISTANCE IN DRY AIR (100 HOUR TEST) FOR HAYNES ALLOY NO. 188 VERSUS HASTELLOY X AND L-605 ALLOYS SHOWING CONTINUOUS PENETRATION FROM ORIGINAL THICKNESS (1)

Alloy	Haynes 188	Hastelloy X	L-605
Test Temp, F	Weight Loss,* mg/cm²		
1600	1.0	1.5	2.1
1800	1.5	2.4	8.5
2000	3.9	5.4	42.4
2100	9.2	9.2	106.1

*Descaled

TABLE 2.0335. OXIDATION WEIGHT LOSS AFTER INTERMITTENT EXPOSURE FOR 100 HOURS IN DRY AIR (BASED ON DESCALED WEIGHT CHANGE) FOR HAYNES ALLOY NO. 188 VERSUS HASTELLOY X AND L-605 ALLOYS (1)

Haynes Alloy No. 188					
Alloy	Exposure Time, hr	Zone Thickness, mils			
		Surface Scale	Intergranular Penetration	Alloy Depletion[a]	Total[b]
Haynes Alloy No. 188	1,000	0.3	1.9	3.2	3.5
	5,000	3.0	3.0	9.0	12.0
	10,000	1.5 (4.0)[c]	5.0	7.0	12.5
L-605	1,000	0.7	3.6	3.6	4.3
	5,000	2.0	4.0	4.0	6.0
	10,000	2.0 (2.0)[c]	4.0	4.0	8.0
Hastelloy X	1,000	0.6	1.7	—	2.3
	5,000	1.3	1.0	3.0	4.3
	10,000	2.0	7.0	7.0	9.0

(a) Depletion of alloy constituents.
(b) Total is surface scale plus maximum of either intergranular penetration or alloy depletion.
(c) Number in parentheses is thickness of scale that spalled.

Note: Specimens were sheet, measuring 0.5 × 1.0 × 0.06 to 0.08 in.

TABLE 2.0336. LONG-TIME OXIDATION BEHAVIOR IN STILL AIR AT 1830 F (34)

	Co
Low	C
22	Cr
22	Ni
14	W
.08	La

Haynes Alloy No. 188

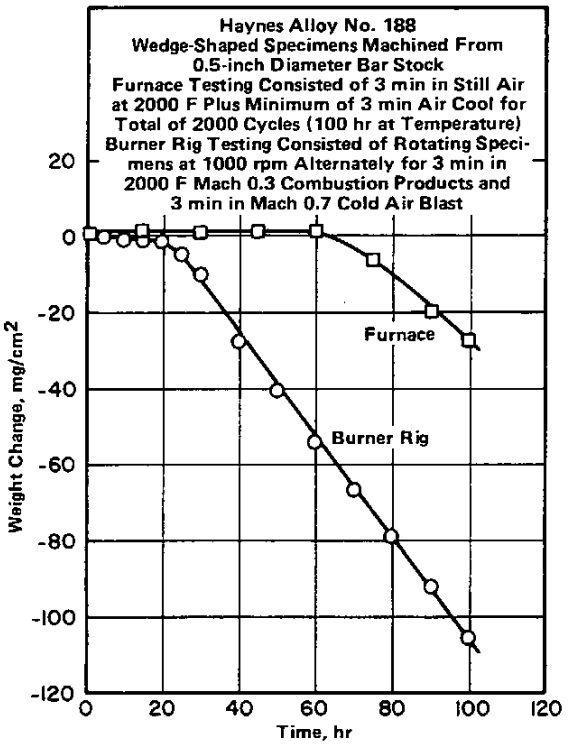

FIGURE 2.0337. OXIDATION WEIGHT CHANGES DURING CYCLIC FURNACE AND BURNER RIG EXPOSURES AT 2000 F (35)

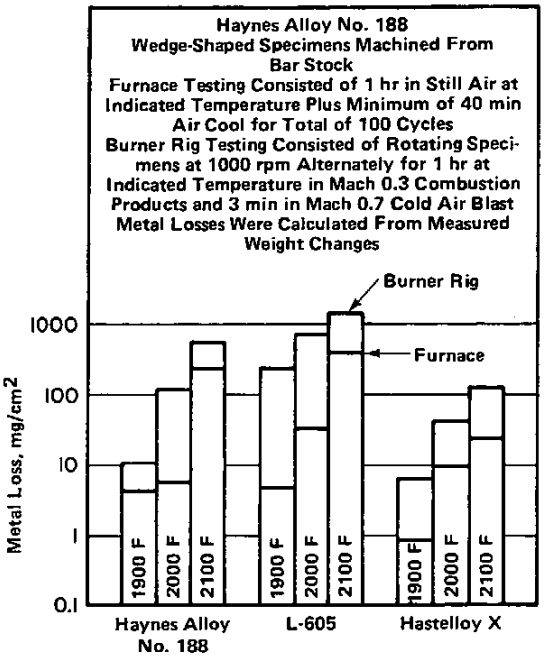

FIGURE 2.0338. CALCULATED METAL LOSSES AFTER CYCLIC FURNACE AND BURNER RIG OXIDATION EXPOSURES FOR 100 HOURS AT 1900 TO 2100 F FOR HAYNES ALLOY NO. 188, L-605, AND HASTELLOY X (35)

	Co
Low	C
22	Cr
22	Ni
14	W
.08	La

Haynes Alloy No. 188

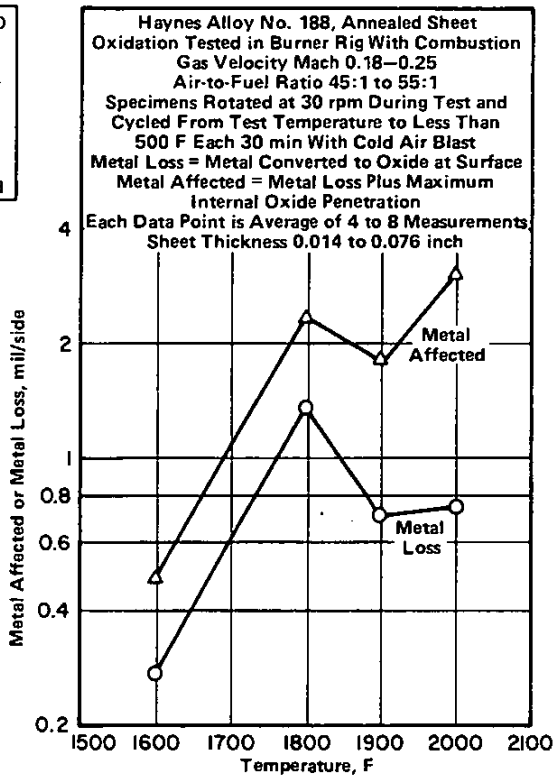

FIGURE 2.0339. DYNAMIC OXIDATION OF HAYNES ALLOY NO. 188 AFTER 100 HOURS AT 1600 TO 2000 F (37)

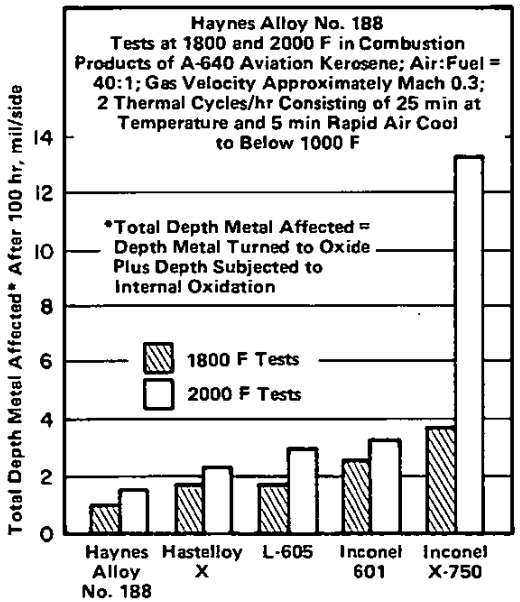

FIGURE 2.03311. OXIDATION RESISTANCE UNDER DYNAMIC CONDITIONS OF HAYNES ALLOY NO. 188 VERSUS OTHER SHEET ALLOYS (11)

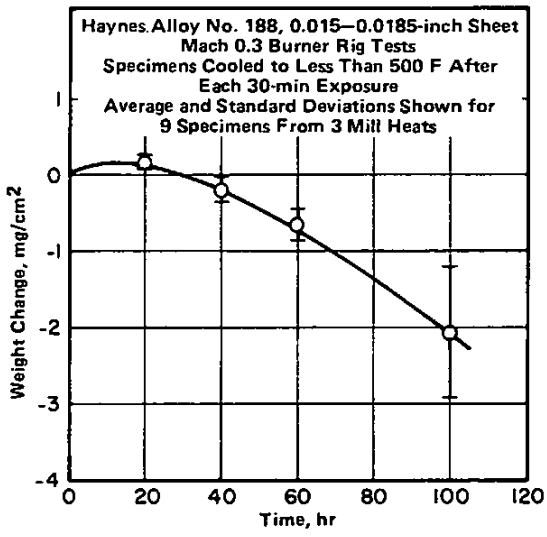

FIGURE 2.03310. DYNAMIC OXIDATION WEIGHT CHANGE BEHAVIOR OF THIN SHEET AT 2000 F (36)

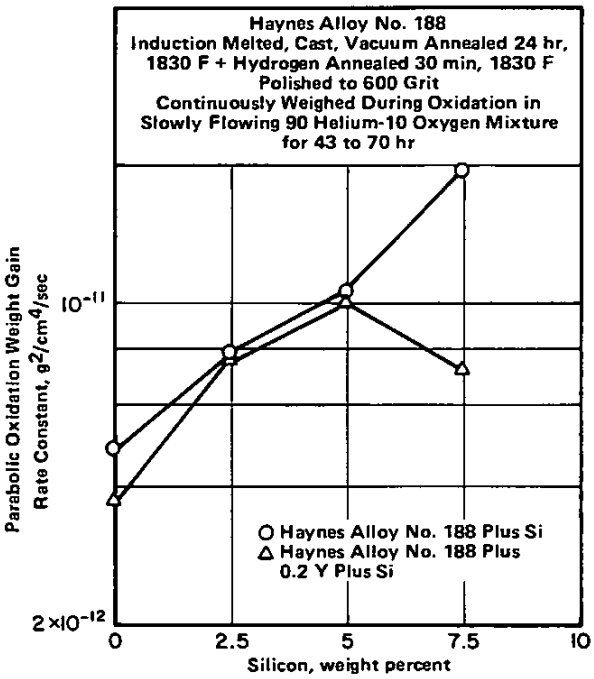

FIGURE 2.03313. EFFECTS OF SILICON AND YTTRIUM ON OXIDATION RATE OF HAYNES ALLOY NO. 188 AT 1830 F (38)

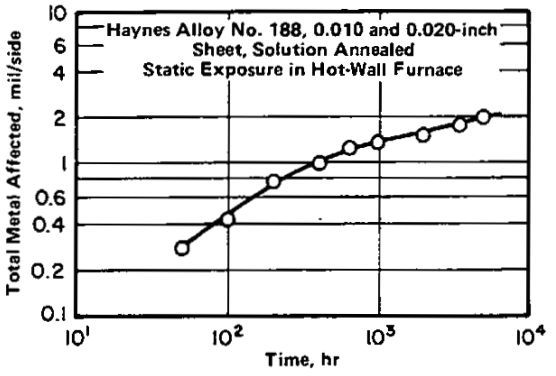

FIGURE 2.03315. OXIDATION BEHAVIOR AT 1800 F AND AIR PRESSURE OF 8 TORR (47)

	Co
Low	C
22	Cr
22	Ni
14	W
.08	La

Haynes Alloy No. 188

Haynes Alloy No. 188							
Temperature, F	Alloy	Total Metal Affected, mils/side[a]					
		Sea Salt, ppm					4 ppm Na_2SO_4
		0	0.5	2	5	10	
1650	S-57	2.4	2.4	2.4	2.4	1.8	3.5
	IN-617	1.3	3.3	4.6	4.6	1.4	4.1
	HA-188	1.8	3.4	4.7	4.7	2.2	5.1
	TD-NiCrAl	0	1.0	12.6	(b)	(b)	2.5
1830	S-57	5.1	5.1	5.1	5.1	6.9	5.6
	IN-617	3.1	4.2	5.6	5.6	8.9	7.7
	HA-188	1.8	2.6	3.5	3.5	7.2	5.9
	TD-NiCrAl	0	0.4	3.1	2.2[c]	0.1[c]	3.1[c]

Test Conditions: Mach 0.3 burner rig, one atmosphere pressure.
Combustion air contained indicated amount of synthetic sea salt or Na_2SO_4
Type A-1 fuel, sulfur content 0.02 to 0.06 weight percent
Air: fuel ratio 20:1 at 1652 and 16:1 at 1832 F
Specimens rotated at 300 rpm
Time at temperature 100 hr. Cycle consisted of 1 hr at temperature and 3 min forced air cooling.

(a) Total metal affected per side = (initial thickness minus final unaffected thickness)/2. Initial thickness about 40 mils for TD-NiCrAl, 80 mils for HA-188 and S-57, and 120 mils for IN-617.
(b) Failed during test in maximum temperature zone.
(c) Failed during test outside maximum temperature zone. Values shown are after 40 hours.

TABLE 2.0342. HOT CORROSION OF HAYNES ALLOY NO. 188 AND THREE OTHER HIGH TEMPERATURE SHEET ALLOYS IN MACH 0.3 BURNER RIG AT 1650 AND 1830 F (40)

	Co
Low	C
22	Cr
22	Ni
14	W
.08	La

Haynes Alloy No. 188

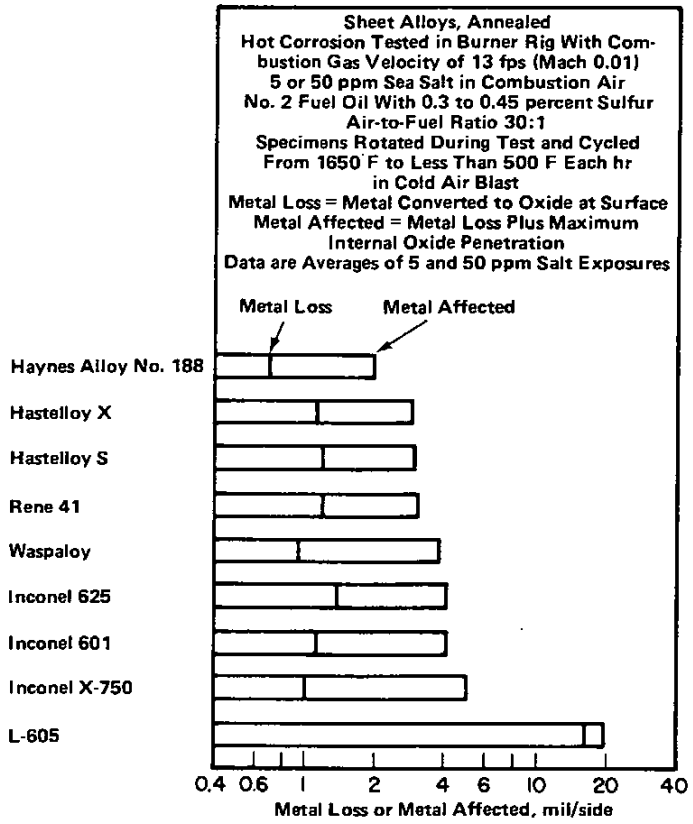

FIGURE 2.0343. HOT CORROSION OF HAYNES ALLOY NO. 188 AND OTHER SHEET SUPERALLOYS AFTER 200 HOURS AT 1650 F (53)

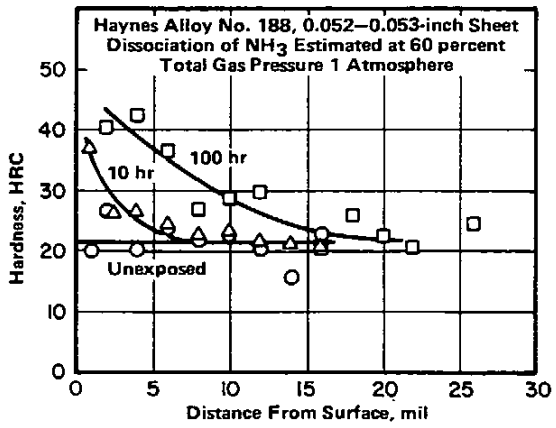

FIGURE 2.0352. CROSS-SECTION HARDNESS CURVES AFTER EXPOSURE TO PARTIALLY DISSOCIATED AMMONIA AT 1800 F (44)

Alloy	Haynes Alloy No. 188		
Form	Sheet, Strip, Plate		Bar, Forgings, Flash Welded Rings
Condition	Solution Heat Treated (2150 F)		
Thickness	≤0.020 in.[a]	>0.020 in.[a]	(b)
Ultimate Strength, F_{tu}, Min, ksi	125	125	125
Yield Strength, F_{ty} Min, ksi	55	55	55
Elongation (2 in. or 4D) Min, percent	40	45	45
Hardness, Brinell, Min	—	—	302 (Bars); 293 (Rings)

(a) Tensile test specimens shall be taken with the axis perpendicular to the direction of rolling from material 9 in. and over in width and with the axis parallel to direction of rolling from material less than 9 in. wide.
(b) Specimens shall be taken in the longitudinal direction from bars, in the circumferential direction from parent metal of flash welded rings, and from forgings in locations as agreed upon by purchaser and vendor.

TABLE 3.011. AMS SPECIFIED MECHANICAL PROPERTIES (3,4)

	Co
Low	C
22	Cr
22	Ni
14	W
.08	La

Haynes Alloy No. 188

Alloy	Haynes Alloy No. 188				
Form	Sheet			Plate	Bar
Condition	Solution Heat Treated – 2150 F				
Thickness, in.	0.010–0.013	0.030–0.065	0.109–0.130	0.250	0.500–1.020
Ultimate Strength, F_{tu} ksi	133	139	137	140	140
Yield Strength, F_{ty} ksi	71	70	68	65	62
Elongation, percent (in 1.125 or 2.0 in.)	56	56	61	52	60
Reduction in Area, percent	—	—	—	—	62

Tested at strain rate of 0.005 in./in./min to 0.6 percent offset and 0.500 in./min crosshead velocity to failure.

TABLE 3.0212. TYPICAL MECHANICAL PROPERTIES AT ROOM TEMPERATURE FOR VARIOUS MILL PRODUCTS (1,14)

Alloy	Haynes Alloy No. 188			
Form	Sheet			All Weld Metal
Condition	As Welded			
Thickness, in.	0.060			~ 1.0
Type of Weld	GTA	Electron Beam (No Filler)	Resistance	GTA
Ultimate Strength, F_{tu}, ksi	124	133	132	117
Yield Strength, F_{ty}, ksi	70	73	71	80
Elongation, percent	31	46	44	39

Sheet was in annealed condition prior to welding and properties were: ultimate strength, = 132.6, yield strength = 68.1, elongation = 65.0 percent.

TABLE 3.0213. TYPICAL MECHANICAL PROPERTIES AT ROOM TEMPERATURE OF WELDED SHEET (1,16)

	Co
Low	C
22	Cr
22	Ni
14	W
.08	La

Haynes Alloy No. 188

Alloy	Haynes Alloy No. 188				
Form	Sheet				
Condition	Mill Annealed + Cold-Rolled*				
Amount of Cold Reduction, percent	10	20	30	40	50
Ultimate Strength F_{tu}, ksi	158	190	212	235	246
Yield Strength, F_{ty}, ksi	130	186	210	216	220
Elongation, percent	43	12	9	6	4

*Sheet thickness was 0.077 inch prior to cold rolling

TABLE 3.0214. EFFECT OF COLD ROLLING AT ROOM TEMPERATURE ON THE MECHANICAL PROPERTIES OF SHEET (1,8,11)

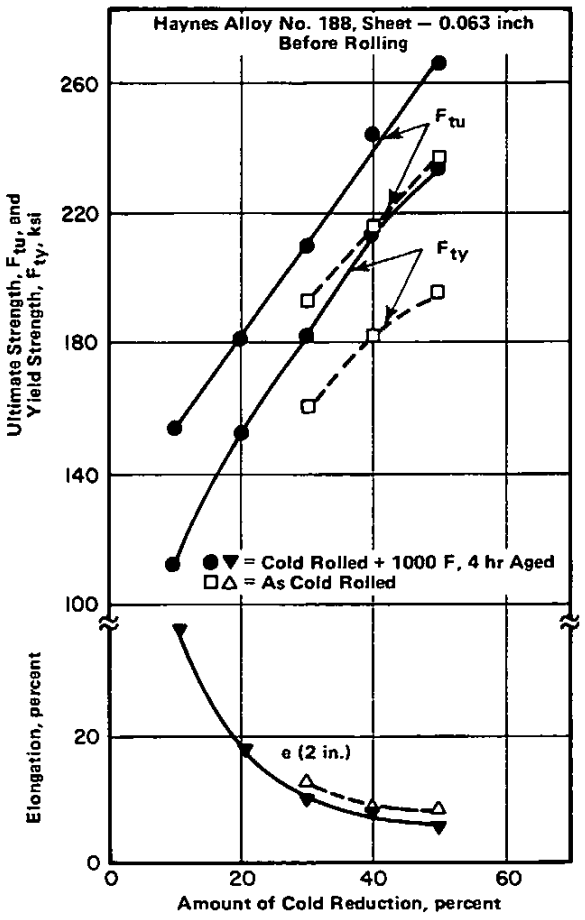

FIGURE 3.0215. EFFECT OF COLD ROLLING FOLLOWED BY AGING ON THE MECHANICAL PROPERTIES OF SHEET (14)

Alloy	Haynes Alloy No. 188			
Form	Sheet			
Thickness, in.	0.043–0.065			
Condition	Solution Annealed + Exposure of 1000 Hr at Indicated Temperature			
Exposure Temp, F	No Exposure	1400	1500	1600
Ultimate Strength, F_{tu}, ksi	138	145	141	132
Yield Strength, F_{ty}, ksi	69	74	71	66
Elongation (in 2 in.), percent	61	37	19	14
HRA	—	64.7	63.7	65.0

Specimen axis was transverse to rolling direction.
Strain rate was 0.005 in./in./min to 0.6 percent offset followed by a constant cross-head velocity of 0.5 in./min to failure.

TABLE 3.0216. EFFECT OF ELEVATED TEMPERATURE EXPOSURE ON THE ROOM TEMPERATURE MECHANICAL PROPERTIES OF SHEET (14)

	Co
Low	C
22	Cr
22	Ni
14	W
.08	La

Haynes Alloy No. 188

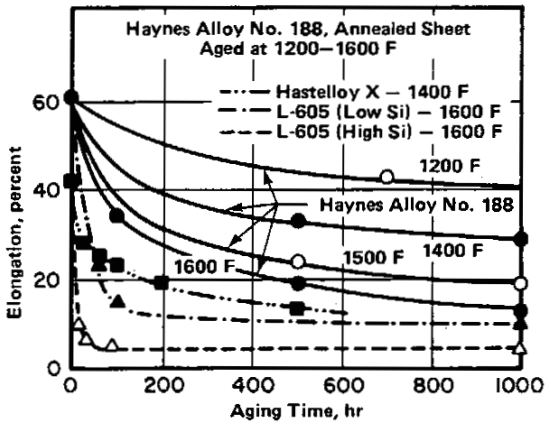

FIGURE 3.0217. EFFECT OF AGING ON ROOM TEMPERATURE ELONGATION OF HAYNES ALLOY NO. 188 VERSUS HASTELLOY X AND L-605 (11)

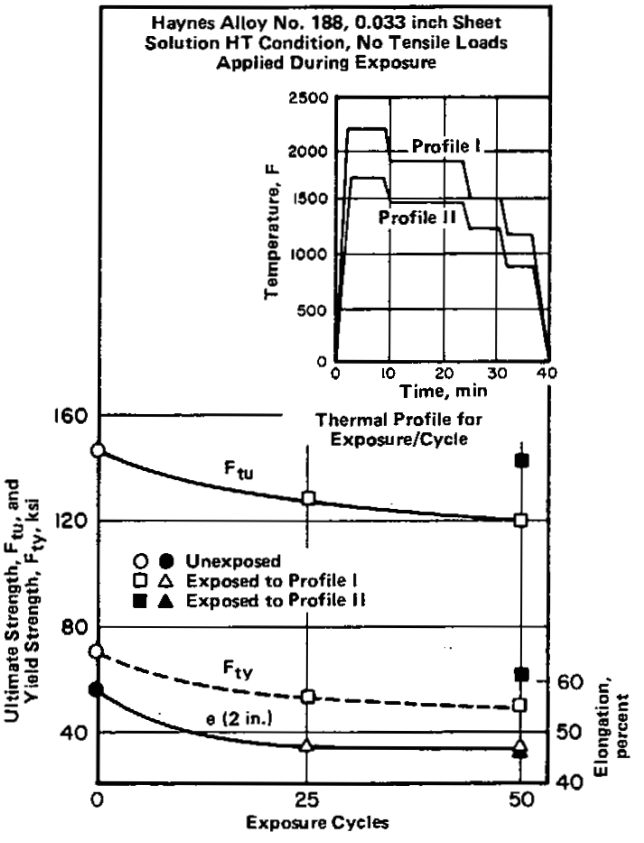

FIGURE 3.0219. EFFECT OF THERMAL CYCLING AT TWO THERMAL PROFILES (INSET) ON ROOM TEMPERATURE PROPERTIES OF EXPOSED SHEET (21)

	Co
Low	C
22	Cr
22	Ni
14	W
.08	La

Haynes Alloy No. 188

Haynes Alloy No. 188							
Exposure Conditions				Post-Exposure Room Temperature Tensile Properties[a]			
Temperature, F[b]	NaCl., mg/cm^2	Stress, ksi	Atmosphere	Ultimate Strength, F_{tu}, ksi	Yield Strength, F_{ty}, ksi	Elongation, percent	Reference
Unexposed				72	148	52	41
				70	148	80	42
1400	0	0	Air	77	141	43	41
	0.15	0	Air	73	132	26.3	
	1.9	0	Air	76	125	16.5	
	2.4	0	Air	80	125	16	
1800	0	0	Air	62	139	44	42
	0	0.8	Air	58	132	48	
	150	0	Air	4	8	0.6	
	150	0.8	Air	33	36	0.6	
	150	0	Air[c]	—	10	0.5	
	150	1.9	Air[c]	Broke During Exposure			
	150	0	Ar-1 percent O	52	93	19	
	150	5.3	Ar-1 percent O	Broke During Exposure			
	150	0	Argon	60	134	62	
	150	1.9	Argon	60	129	37	

(a) Flat sheet tensile specimens, 0.015 (Ref. 41) or 0.020 (Ref. 42) in. thick. Materials initially annealed for 1 hr at 2150 or 2175 F.

(b) Exposed for 48 hr at indicated temperature.

(c) Preoxidized in air for 2 hr at 1720 F before salt coating.

TABLE 3.02110. EFFECTS OF SALT ON POST-EXPOSURE TENSILE PROPERTIES AT ROOM TEMPERATURE (41,42)

Alloy	Haynes Alloy No. 188					
Form	Plate					
Thickness, in.	0.750					
Condition	2150 F, Water Quench + Exposure as Indicated					
Expsosure Time, hr	None	100	100	500	1000	100
Exposure Temp, F	None	1400	1600	1700	1700	1800
Impact Strength, ft-lb IE Charpy V						
Longitudinal	145	—	—	23	17	—
Transverse	140	39	35	26	17	31

Exposure (aging treatment) performed in vacuum.

TABLE 3.0231. IMPACT STRENGTH OF PLATE AT ROOM TEMPERATURE IN THE SOLUTION TREATED CONDITION AND AFTER ELEVATED TEMPERATURE EXPOSURE (1,11)

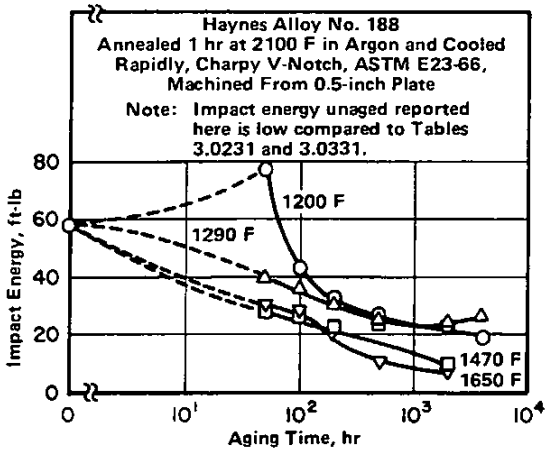

FIGURE 3.0232. EFFECTS OF AGING AT ELEVATED TEMPERATURES ON NOTCH-IMPACT ENERGY AT ROOM TEMPERATURE (54)

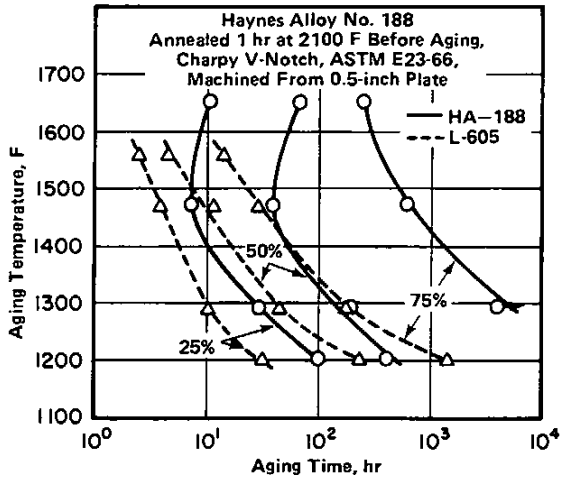

	Co
Low	C
22	Cr
22	Ni
14	W
.08	La

Haynes Alloy No. 188

FIGURE 3.0233. AGING TIME-TEMPERATURE CURVES FOR 25, 50, AND 75 PERCENT REDUCTIONS IN NOTCH-IMPACT ENERGY AT ROOM TEMPERATURE FOR HAYNES ALLOY NO. 188 AND L-605 (54)

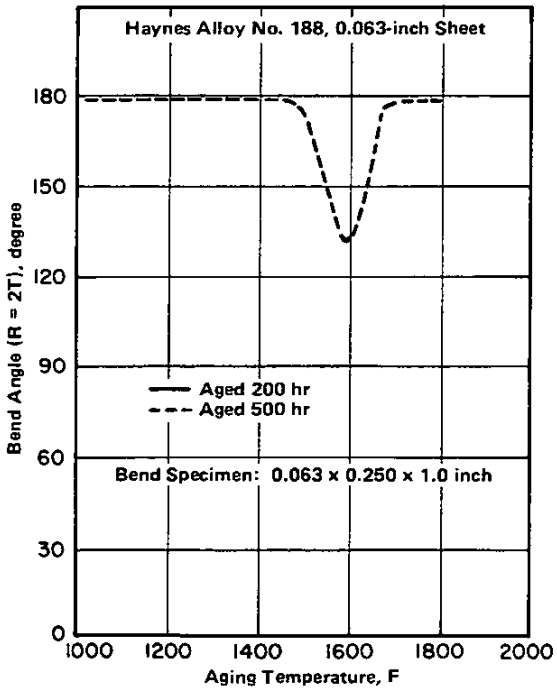

FIGURE 3.0241. BEND DUCTILITY OF AGED SHEET (6)

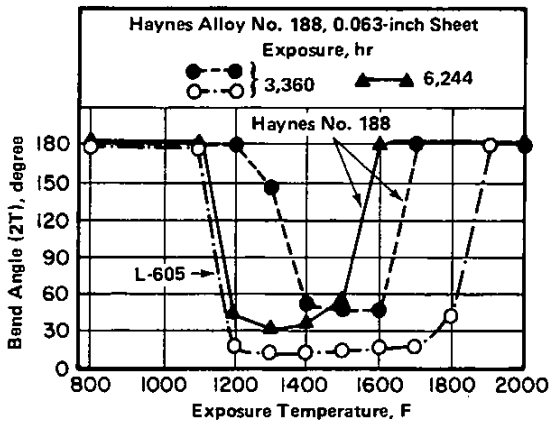

FIGURE 3.0242. EFFECT OF ELEVATED TEMPERATURE EXPOSURE ON BEND DUCTILITY OF HAYNES ALLOY NO. 188 AND L-605 SHEET (6)

	Co
Low	C
22	Cr
22	Ni
14	W
.08	La

Haynes Alloy No. 188

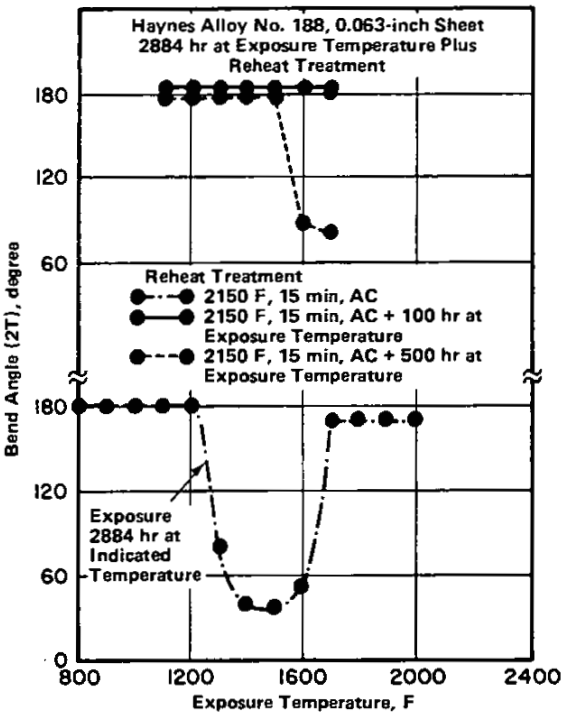

FIGURE 3.0243. EFFECT OF SUBSEQUENT RESOLUTION HEAT TREATMENT AND ADDITIONAL AGING (TOP GRAPH) ON BEND DUCTILITY OF SHEET PREVIOUSLY SUBJECTED TO ELEVATED TEMPERATURE EXPOSURE (BOTTOM GRAPH) (6)

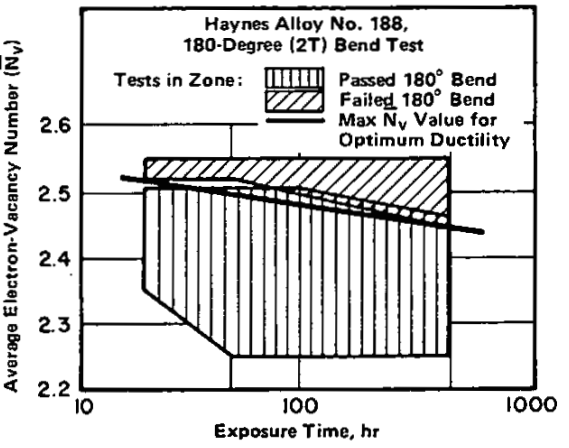

FIGURE 3.0244. EFFECT OF AVERAGE ELECTRON-VACANCY NUMBER (N_v), DETERMINED FROM CHEMICAL COMPOSITION, ON BEND DUCTILITY OF SHEET AFTER EXPOSURE AT 1600 F (6)

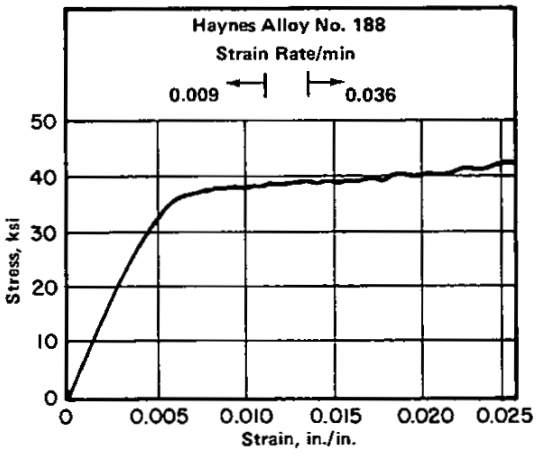

FIGURE 3.03111. STRESS-STRAIN CURVE AT 1600 F (14)

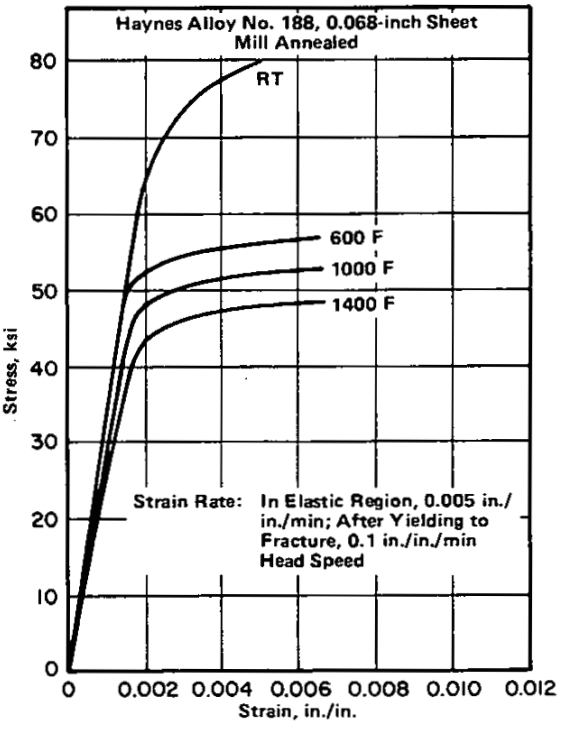

FIGURE 3.03112. TYPICAL STRESS-STRAIN CURVES FOR SHEET TESTED IN THE LONGITUDINAL DIRECTION AT ROOM AND ELEVATED TEMPERATURES (29)

	Co
Low	C
22	Cr
22	Ni
14	W
.08	La

Haynes Alloy No. 188

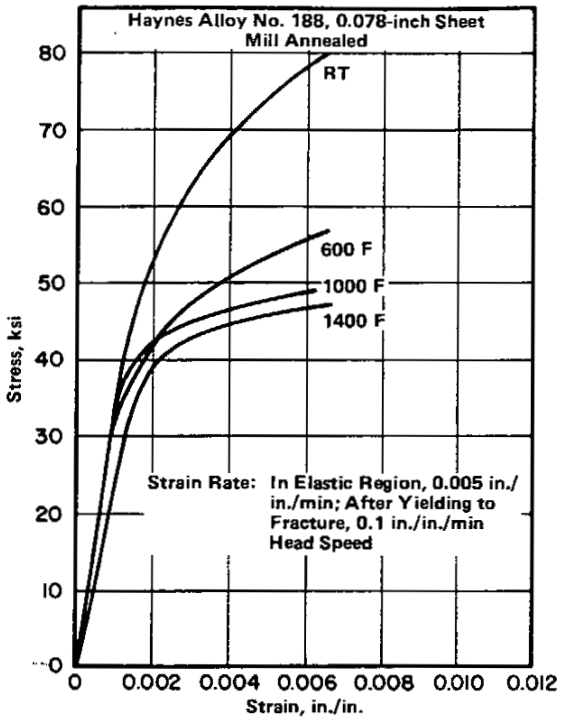

FIGURE 3.03113. TYPICAL STRESS-STRAIN CURVES FOR SHEET TESTED IN THE TRANSVERSE DIRECTION AT ROOM AND ELEVATED TEMPERATURES (29)

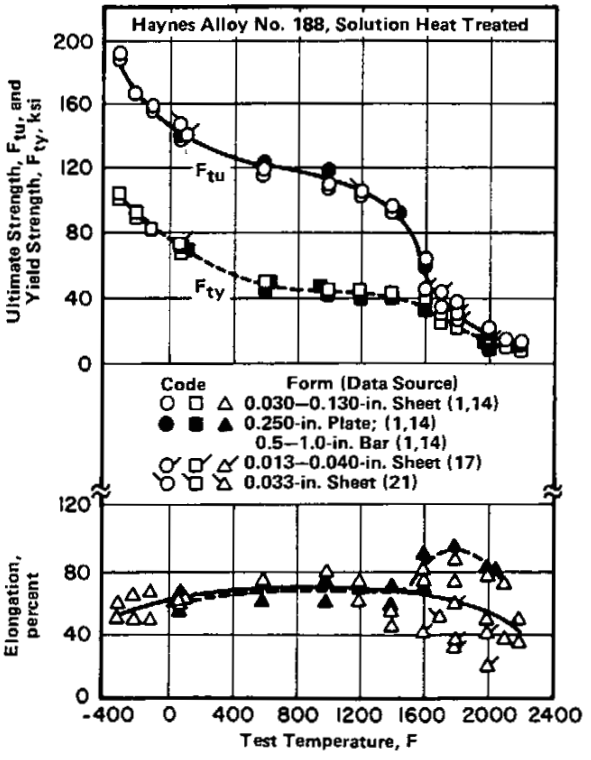

FIGURE 3.0312. EFFECT OF TEST TEMPERATURE ON TENSILE PROPERTIES OF SHEET, PLATE, AND BAR (1,14,17,21)

	Co
Low	C
22	Cr
22	Ni
14	W
.08	La

Haynes Alloy No. 188

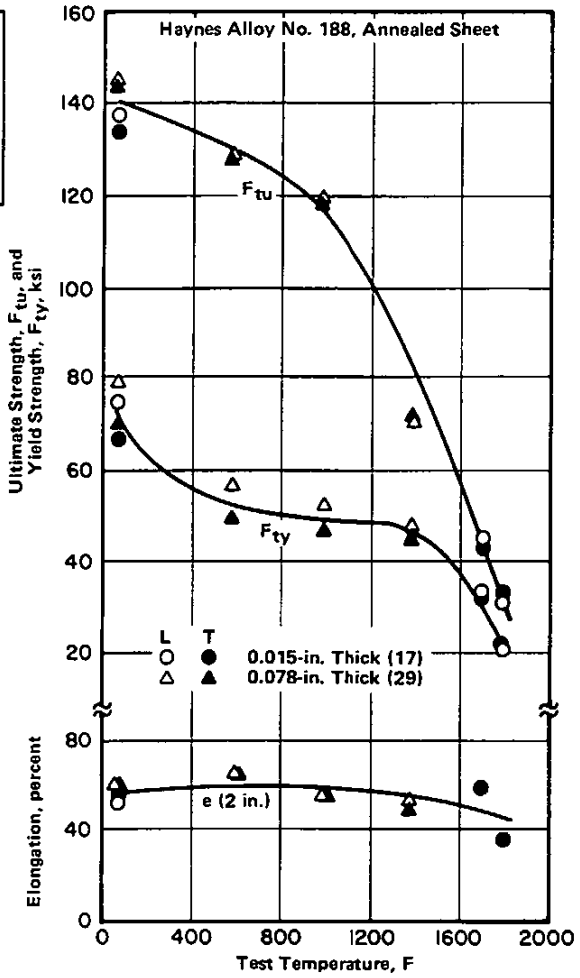

FIGURE 3.0313. EFFECT OF TEST TEMPERATURE ON TENSILE PROPERTIES OF SHEET TESTED IN THE LONGITUDINAL AND TRANSVERSE DIRECTIONS (17,29)

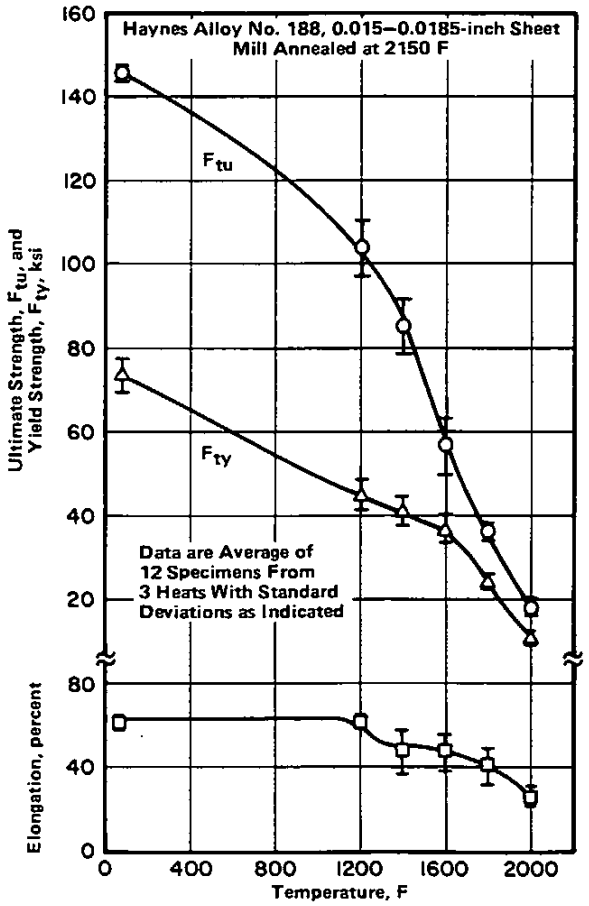

FIGURE 3.0314. EFFECT OF TEMPERATURE ON AVERAGE TENSILE PROPERTIES OF THIN SHEET TESTED IN THE LONGITUDINAL AND TRANSVERSE DIRECTIONS (36)

	Co
Low	C
22	Cr
22	Ni
14	W
.08	La

Haynes Alloy No. 188

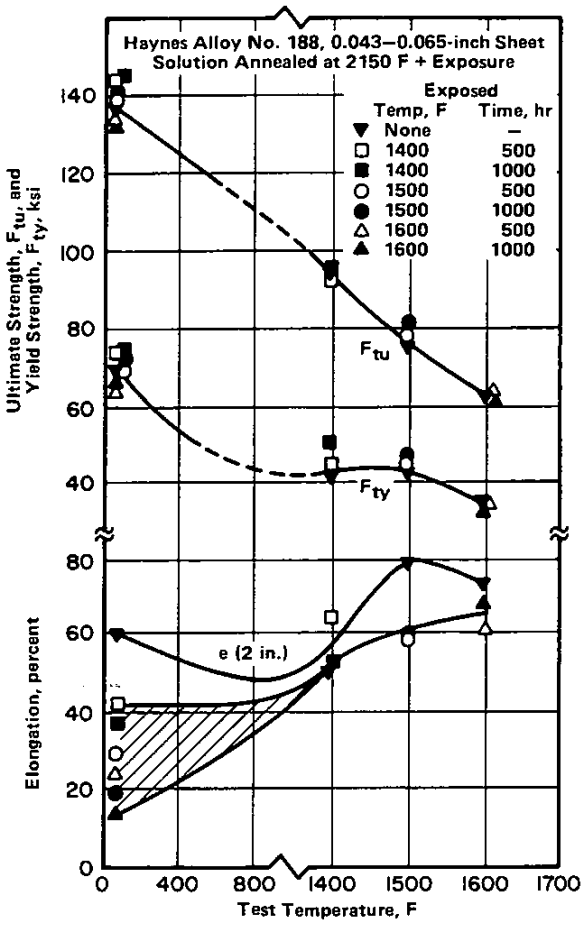

FIGURE 3.0315. EFFECT OF TEST TEMPERATURE ON TENSILE PROPERTIES OF SHEET AFTER EXPOSURE AT ELEVATED TEMPERATURES (14)

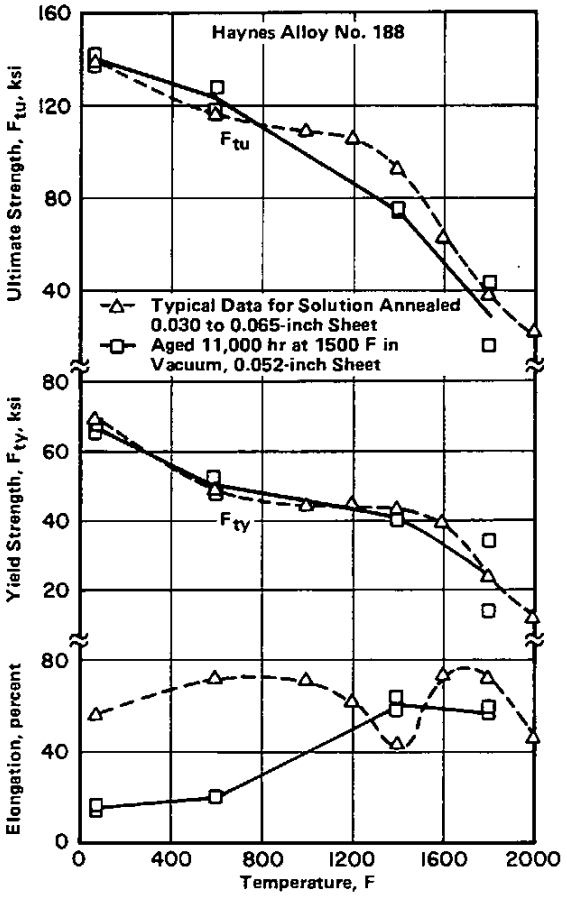

FIGURE 3.0316. EFFECT OF TEST TEMPERATURE ON TENSILE PROPERTIES OF SHEET AFTER LONG-TIME EXPOSURE AT 1500 F (55)

	Co
Low	C
22	Cr
22	Ni
14	W
.08	La

Haynes Alloy No. 188

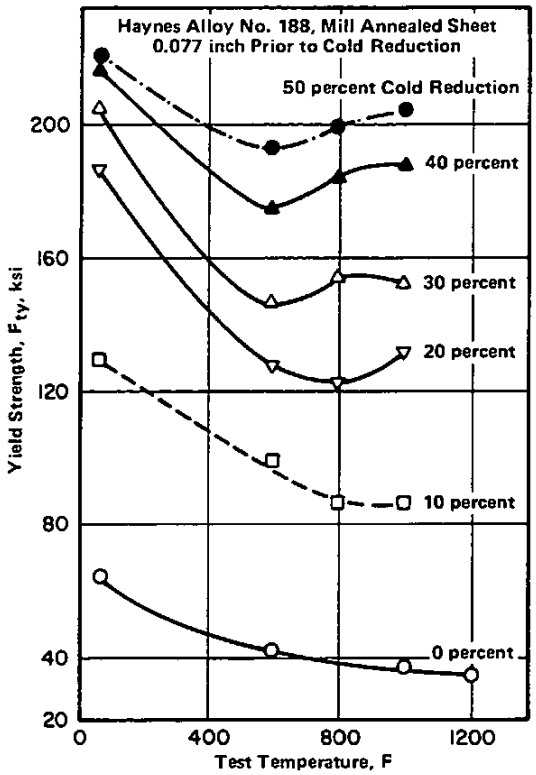

FIGURE 3.0317. EFFECT OF TEST TEMPERATURE ON YIELD STRENGTH OF COLD ROLLED SHEET (1,8,11)

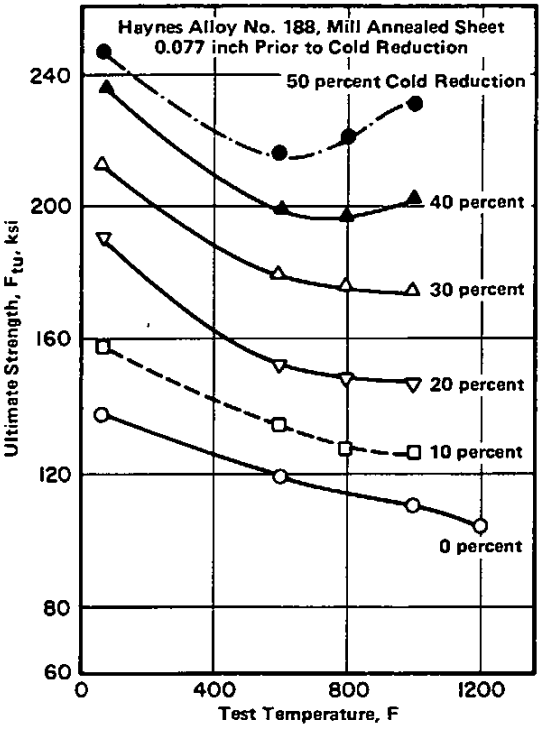

FIGURE 3.0318. EFFECT OF TEST TEMPERATURE ON THE ULTIMATE TENSILE STRENGTH OF COLD ROLLED SHEET (1,8,11)

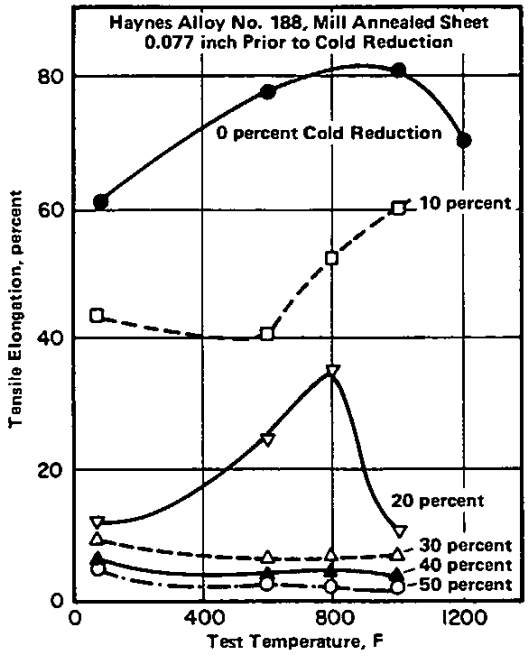

FIGURE 3.0319. EFFECT OF TEST TEMPERATURE IN THE TENSILE ELONGATION OF COLD ROLLED SHEET (1,8,11)

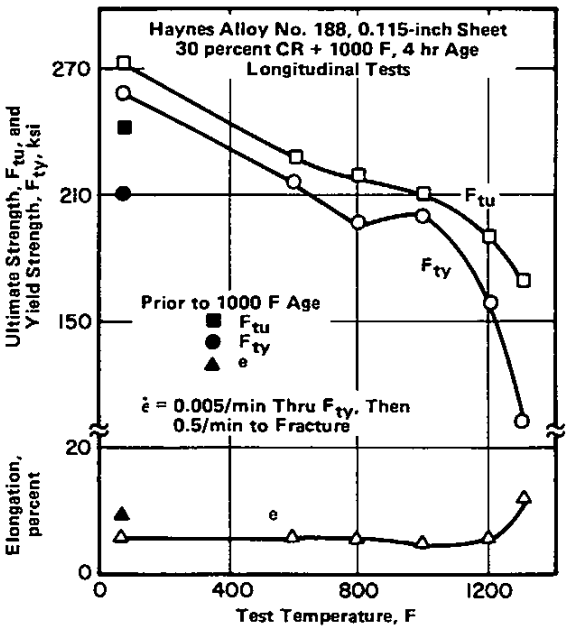

FIGURE 3.03110. EFFECT OF TEST TEMPERATURE ON TENSILE PROPERTIES OF 30 PERCENT COLD ROLLED AND AGED SHEET (18)

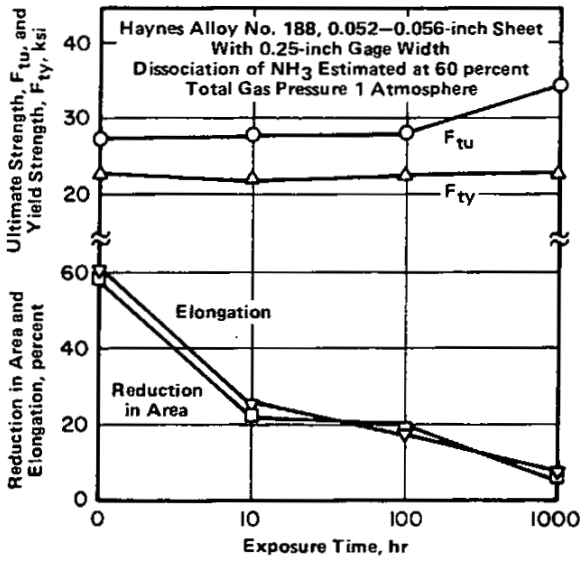

FIGURE 3.03111. TENSILE PROPERTIES OF HAYNES ALLOY NO. 188 AT 1800 F AFTER EXPOSURE TO PARTIALLY DISSOCIATED AMMONIA AT 1800 F (44)

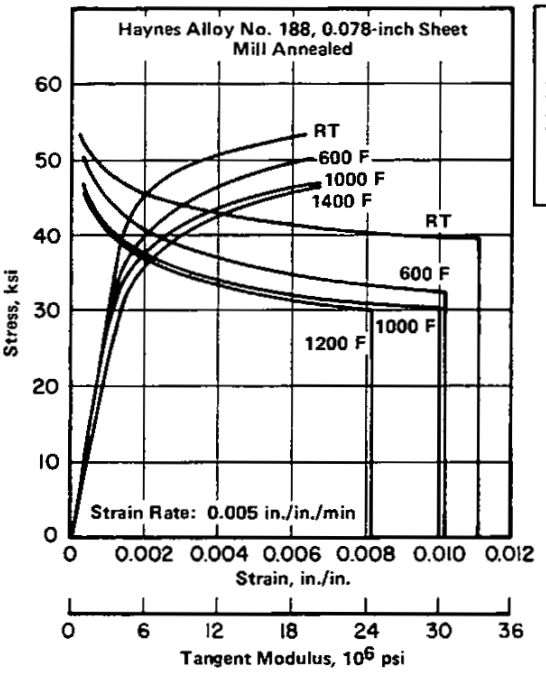

	Co
Low	C
22	Cr
22	Ni
14	W
.08	La

Haynes Alloy No. 188

FIGURE 3.03211. TYPICAL COMPRESSION STRESS-STRAIN AND TANGENT MODULUS CURVES FOR SHEET TESTED IN THE LONGITUDINAL DIRECTION AT ROOM AND ELEVATED TEMPERATURES (29)

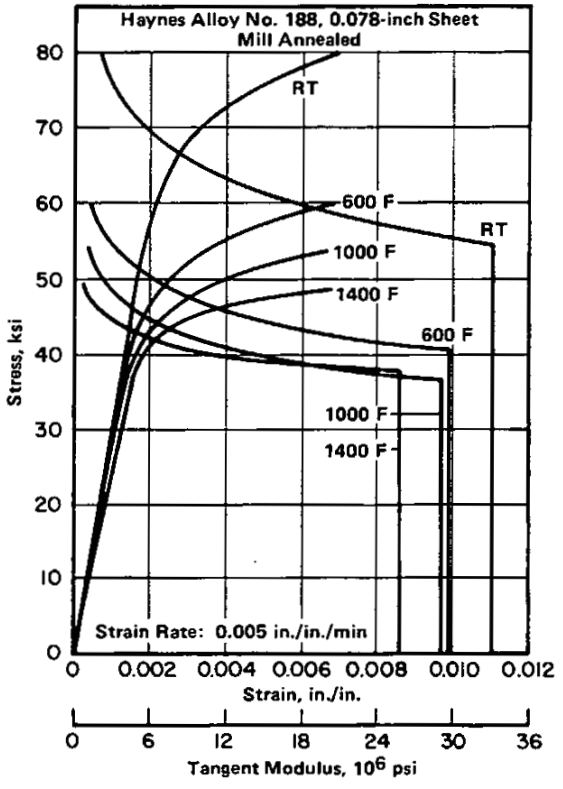

FIGURE 3.03212. TYPICAL COMPRESSION STRESS-STRAIN AND TANGENT MODULUS CURVES FOR SHEET TESTED IN THE TRANSVERSE DIRECTION AT ROOM AND ELEVATED TEMPERATURES (29)

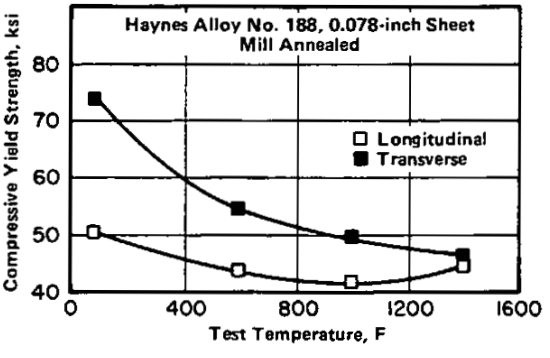

FIGURE 3.03213. EFFECT OF TEST TEMPERATURE ON THE COMPRESSIVE YIELD STRENGTH OF SHEET TESTED IN THE LONGITUDINAL AND TRANSVERSE DIRECTIONS (29)

	Co
Low	C
22	Cr
22	Ni
14	W
.08	La

Haynes Alloy No. 188

Alloy	Haynes Alloy No. 188	
Form	0.750-in. Plate	
Condition	Solution Annealed at 2150 F, WQ	
	Impact Strength, ft-lb— IE Charpy V	
Test Temp, F	Longitudinal	Transverse
−300	117	115
−270	120	—
−220	—	112
−150	134	127
Room	145	140
600	101	—
1000	108	126
1300	126	87
1500	104	—

TABLE 3.0331. EFFECT OF TEST TEMPERATURE ON IMPACT STRENGTH OF PLATE (1)

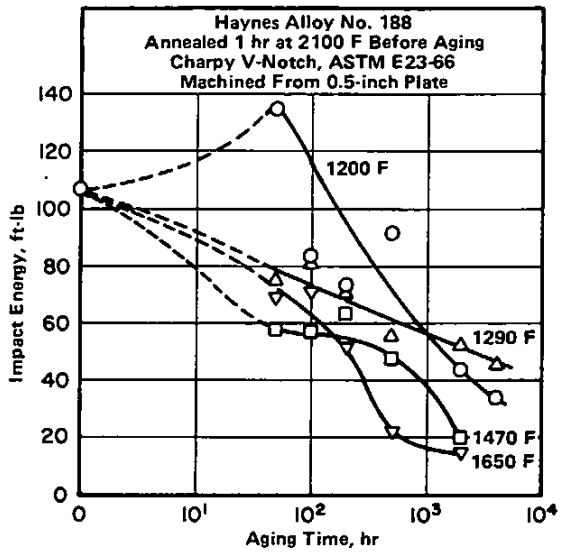

FIGURE 3.0332. EFFECTS OF AGING ON ELEVATED TEMPERATURES ON NOTCH-IMPACT ENERGY AT 570 F (54)

Haynes Alloy No. 188			
Temperature, F	Pre-Braze Cleaning Procedure[a]	Ultimate Shear Strength, ksi[b]	Failure Location
70	A	14.55	Braze Joint
		14.85	Braze Joint
		14.23	Braze Joint
	B	13.04	Braze Joint
		13.77	Braze Joint
		14.42	Braze Joint
	C	12.86	Braze Joint
		13.27	Braze Joint
		16.77	Braze Joint
1800	A	7.34	Base Metal
		7.09	Base Metal
		7.32	Base Metal
	B	7.32	Braze Joint
		7.12	Braze Joint
		7.48	Base Metal
	C	7.37	Base Metal
		7.08	Braze Joint
		7.05	Base Metal

Brazed with AMS 4782 (Nicrobraze 30) in vacuum for 10 min at 2150 to 2175 F.

(a) A—acetone cleaned; B—chemically cleaned; C—chemically milled and chemically cleaned.

(b) Based on overlap braze area about 1-in. wide and 0.1-in. long. Base alloy sheet thickness was 0.020 inch.

TABLE 3.0351. LAP-SHEAR STRENGTH OF BRAZED JOINTS (56,57)

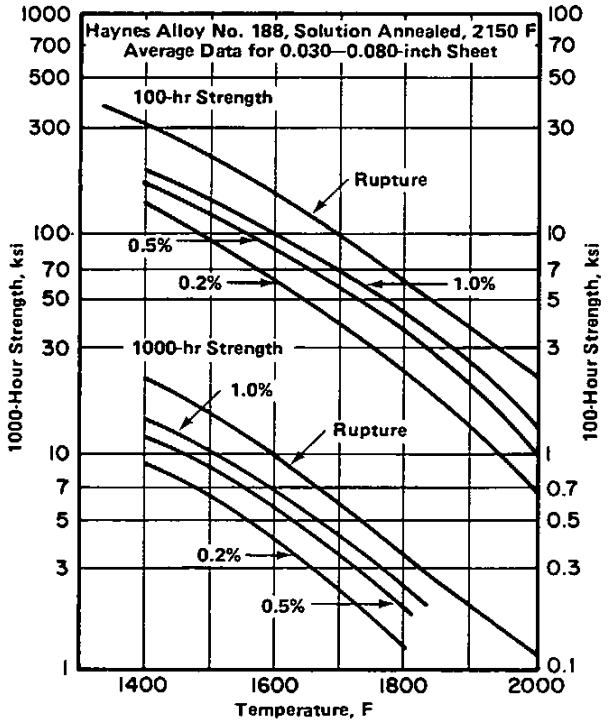

FIGURE 3.041. CREEP STRAIN AND CREEP-RUPTURE CURVES FOR 100- AND 1000-HOUR LIFE OF SHEET AT 1400 TO 2000 F (11,13)

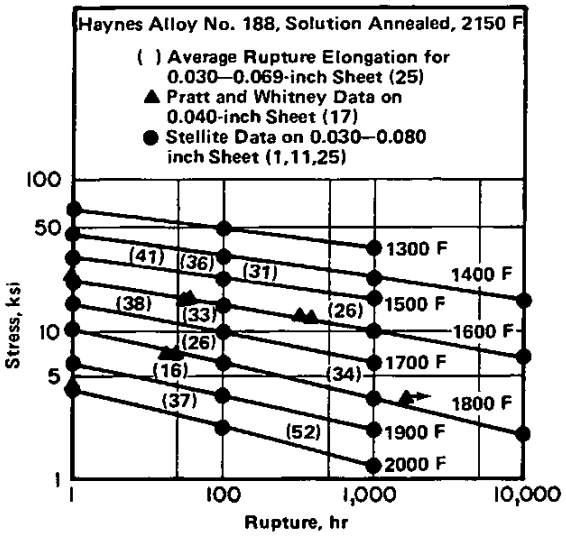

FIGURE 3.042. CREEP-RUPTURE CURVES AT 1300 TO 2000 F FOR SOLUTION HEAT TREATED SHEET (1,11,17,25)

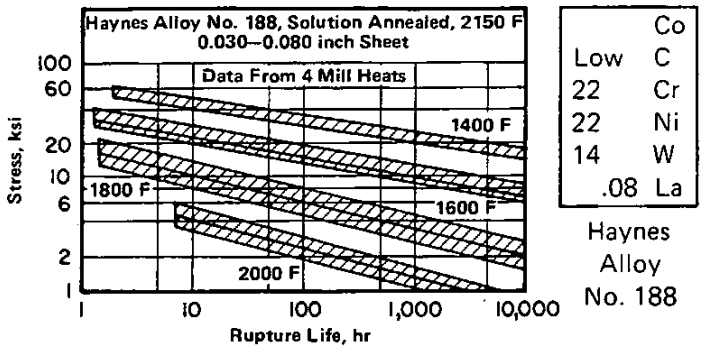

FIGURE 3.043. CREEP-RUPTURE CURVES AT 1400 TO 2000 F FOR SHEET TESTED IN LONGITUDINAL AND TRANSVERSE DIRECTIONS (19)

Alloy	Haynes Alloy No. 188				
Form	Sheet - 20 Heats				
Condition	Solution Annealed, 2150 F				
Test Temp, F	1500	1500	1700	1900	2000
Stress, ksi	25.0	24.0	13.0	4.5	3.2
Number of Tests	76	55	67	55	73
Avg Life, hr	45	61	26	44	21

TABLE 3.044. AVERAGE CREEP RUPTURE LIFE AT 1500 TO 2000 F OF 20 PRODUCTION HEATS OF SHEET BASED ON SHORT-TIME QUALITY CONTROL TESTS (19)

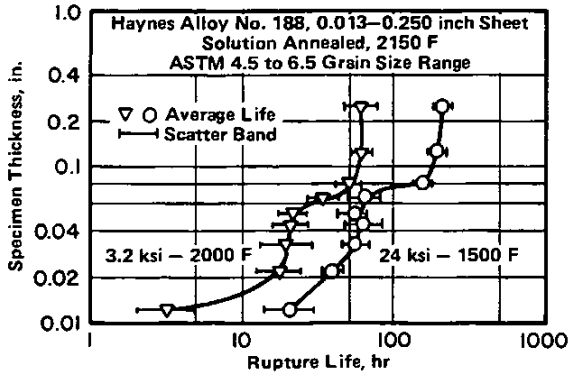

FIGURE 3.045. EFFECT OF SHEET THICKNESS ON RUPTURE LIFE AT 1500 AND 2000 F (14)

	Co
Low	C
22	Cr
22	Ni
14	W
.08	La

Haynes Alloy No. 188

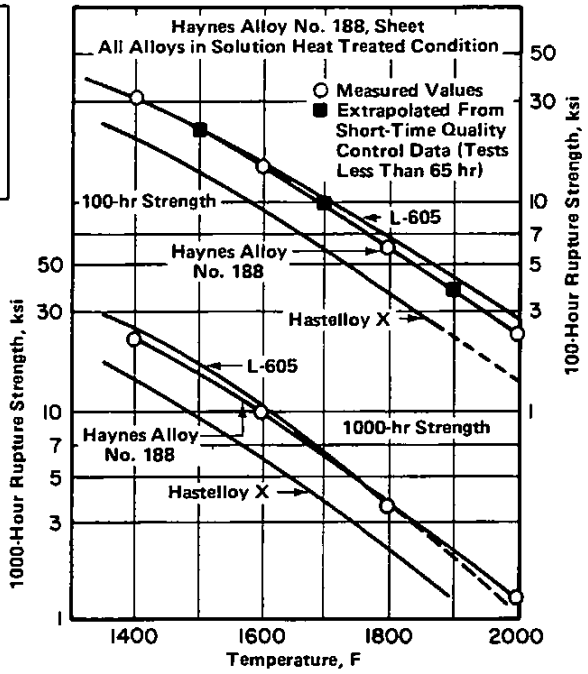

FIGURE 3.046. COMPARISON OF 100- AND 1000-HOUR CREEP-RUPTURE LIFE OF HAYNES ALLOY NO. 188 SHEET AT 1400 TO 2000 F WITH L-605 AND HASTELLOY X SHEET (19)

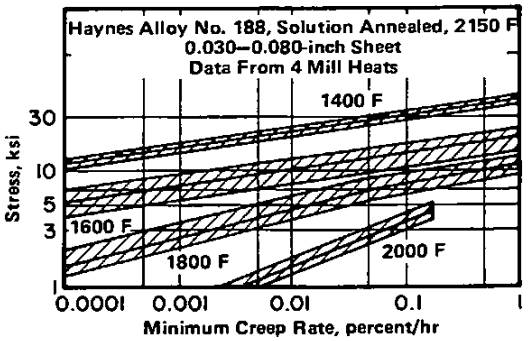

FIGURE 3.047. EFFECT OF STRESS AND TEMPERATURE ON MINIMUM CREEP RATE OF SHEET (19)

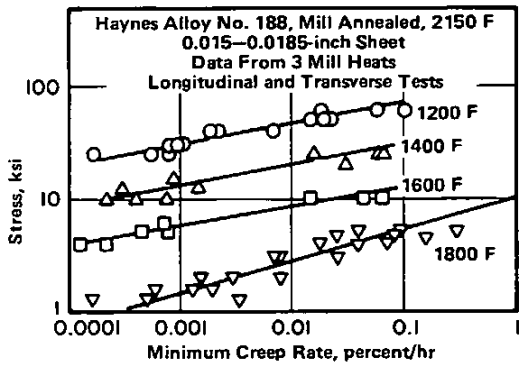

FIGURE 3.048. EFFECT OF STRESS AND TEMPERATURE ON MINIMUM CREEP RATE OF THIN SHEET (36)

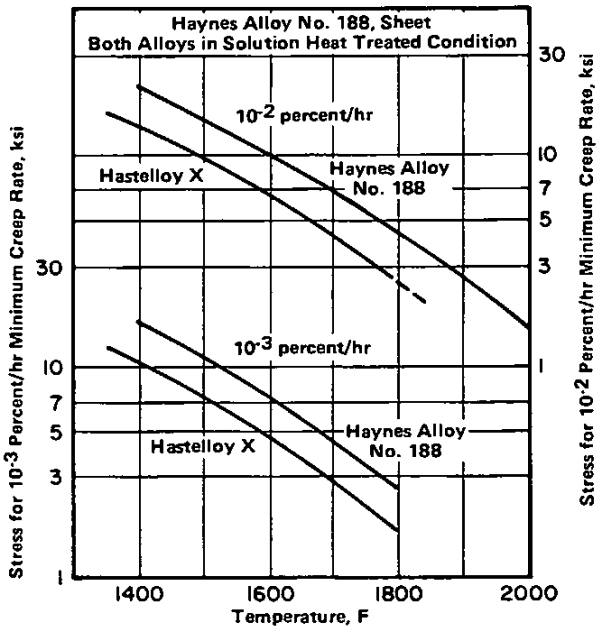

FIGURE 3.049. COMPARISON OF MINIMUM CREEP RATE STRESSES OF HAYNES ALLOY NO. 188 SHEET AT 1400 TO 1800 F WITH HASTELLOY X SHEET (19)

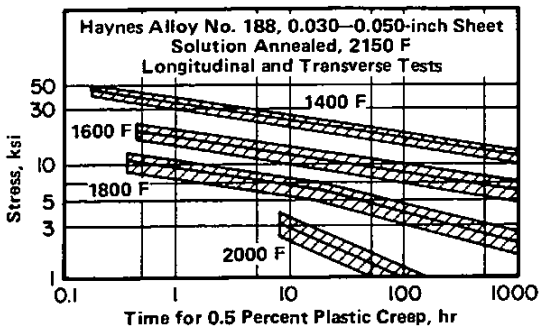

FIGURE 3.0410. STRESS VERSUS 0.5 PERCENT CREEP CURVES FOR SHEET AT 1400 TO 2000 F (19)

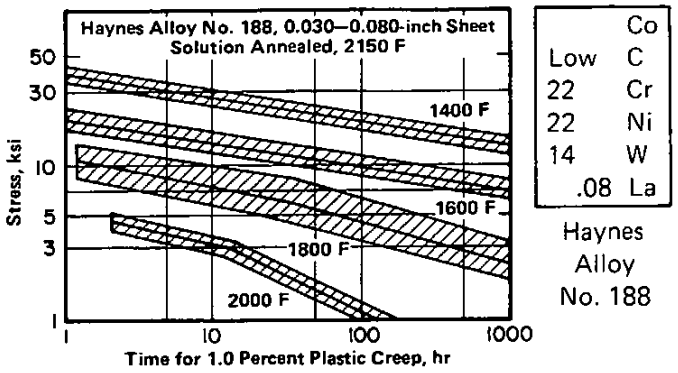

FIGURE 3.0411. STRESS VERSUS 1.0 PERCENT CREEP CURVES FOR SHEET AT 1400 TO 2000 F (19)

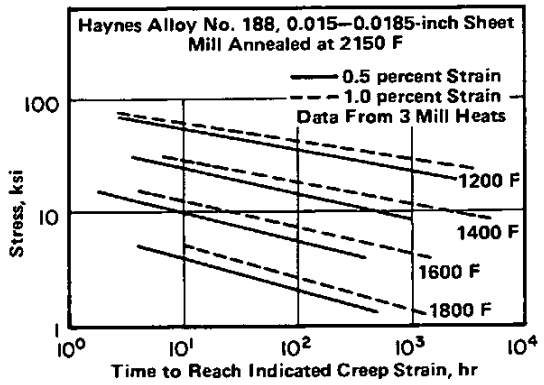

FIGURE 3.0412. AVERAGE CREEP-STRAIN CURVES AT 1200 TO 1800 F FOR THIN SHEET TESTED IN LONGITUDINAL AND TRANSVERSE DIRECTIONS (36)

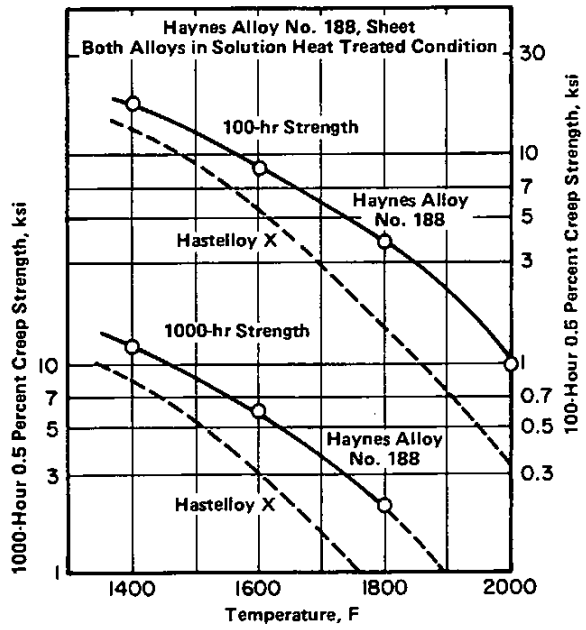

FIGURE 3.0413. COMPARISON OF 100- AND 1000-HOUR 0.5 PERCENT CREEP STRENGTH OF HAYNES ALLOY NO. 188 SHEET AT 1400 TO 2000 F WITH HASTELLOY X SHEET (19)

	Co
Low	C
22	Cr
22	Ni
14	W
.08	La

Haynes Alloy No. 188

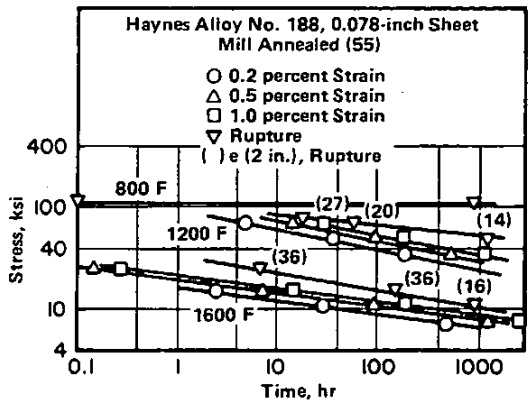

FIGURE 3.0414. CREEP-STRAIN AND CREEP-RUPTURE CURVES FOR SHEET AT 800 TO 1600 F TESTED IN THE TRANSVERSE DIRECTION (29)

Haynes Alloy No. 188		
Grain Size	Average Time to Indicated Creep Strain, hr	
	0.5 percent	1.0 percent
ASTM 2-4	22.8	62.2
ASTM 5-6	19.0	44.3
ASTM 6-6½	19.1	42.8
ASTM 7-8	8.1	16.0

TABLE 3.0415. EFFECT OF GRAIN SIZE ON CREEP LIFE OF 15-MIL SHEET AT 1700 F AND 6 KSI (36,58)

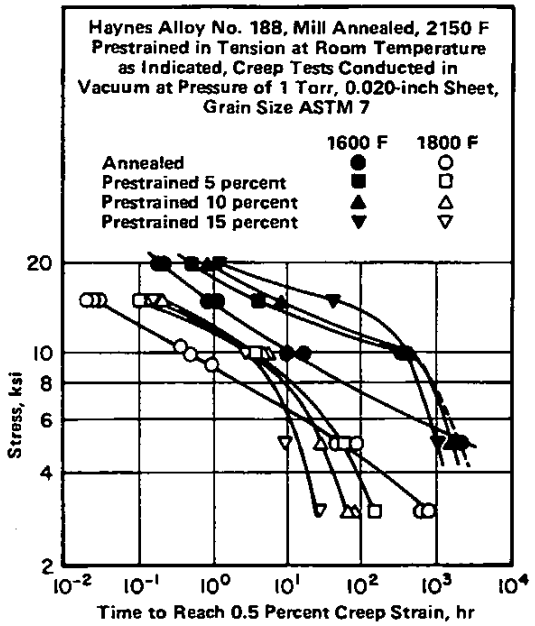

FIGURE 3.0417. EFFECT OF PRESTRAINING AT ROOM TEMPERATURE ON 0.5 PERCENT CREEP STRAIN CURVES AT 1600 AND 1800 F (59)

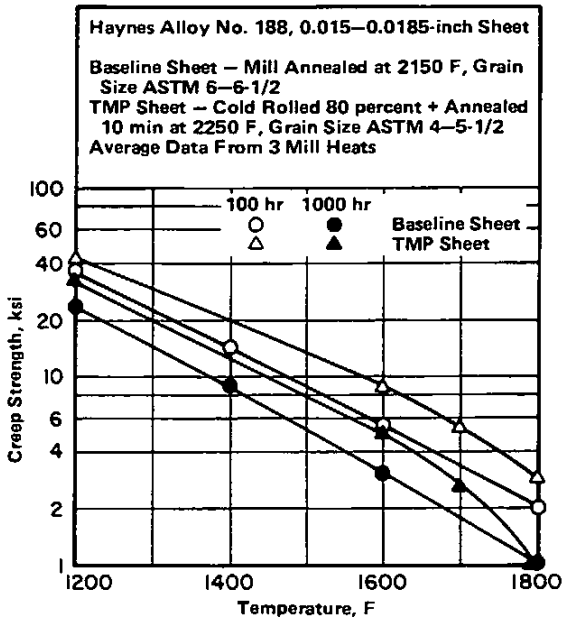

FIGURE 3.0418. EFFECT OF THERMAL-MECHANICAL PROCESSING ON 0.5 PERCENT CREEP STRENGTH OF THIN SHEET AT 1200 TO 1800 F (36)

Haynes Alloy No. 188[a]				
NaCl, mg/cm^2	Test Atmosphere	Creep Rate, percent/hr	Rupture Life, hr	Elongation, percent
0	Air	~ 0.04	136	29
150	Argon	0.058	83.5	9.7
150	Ar-1 percent O	0.058	24.7	4.3
150	Air	1.0	2.2	4.0

(a) Flat sheet specimens, 0.020 in. thick. Specimens were annealed 1 hr at 2175 F before coating with salt.

TABLE 3.0419. EFFECTS OF SALT AND TEST ATMOSPHERE ON CREEP-RUPTURE PROPERTIES AT 1800 F AND 5.25 KSI (42)

	Co
Low	C
22	Cr
22	Ni
14	W
.08	La

Haynes Alloy No. 188

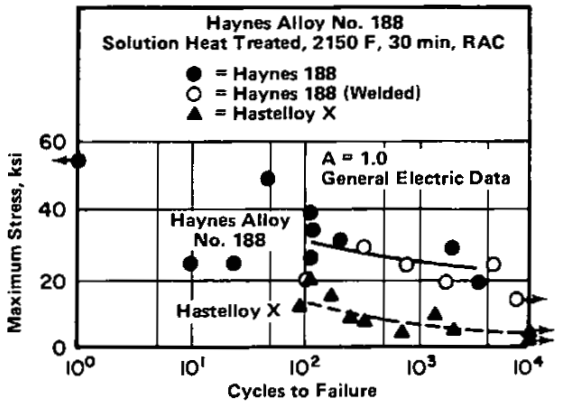

FIGURE 3.051. LOW CYCLE FATIGUE DATA AT 1700 F FOR HAYNES ALLOY NO. 188, HASTELLOY X AND GTA-WELDED HAYNES ALLOY NO. 188 (20)

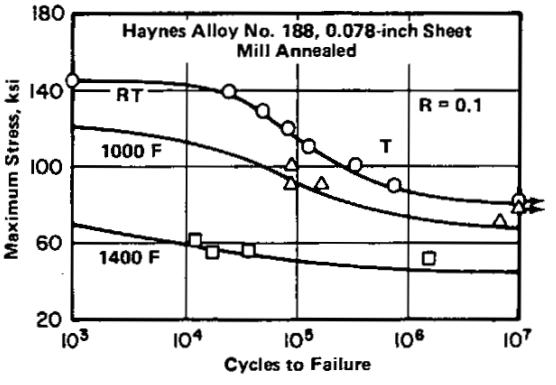

FIGURE 3.052. AXIAL-LOAD FATIGUE STRENGTH OF UNNOTCHED SHEET AT ROOM AND ELEVATED TEMPERATURES TESTED IN THE TRANSVERSE DIRECTION (29)

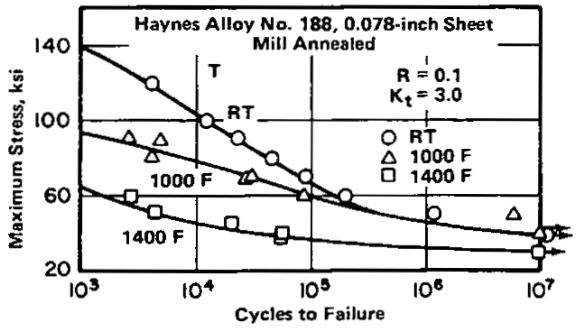

FIGURE 3.053. AXIAL-LOAD FATIGUE STRENGTH OF NOTCHED SHEET AT ROOM AND ELEVATED TEMPERATURES TESTED IN THE TRANSVERSE DIRECTION (29)

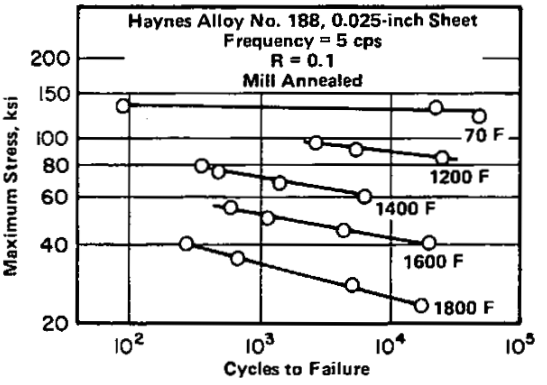

FIGURE 3.054. AXIAL-LOAD FATIGUE STRENGTH OF UNNOTCHED THIN SHEET AT ROOM AND ELEVATED TEMPERATURES TESTED IN THE LONGITUDINAL DIRECTION (60)

	Co
Low	C
22	Cr
22	Ni
14	W
.08	La

Haynes Alloy No. 188

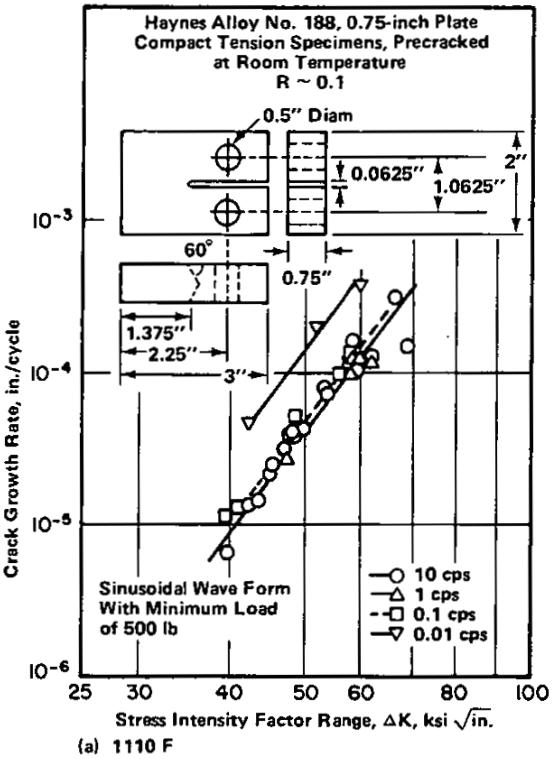

(a) 1110 F

FIGURE 3.056. FATIGUE CRACK GROWTH RATES AT 1110 TO 1600 F (49)

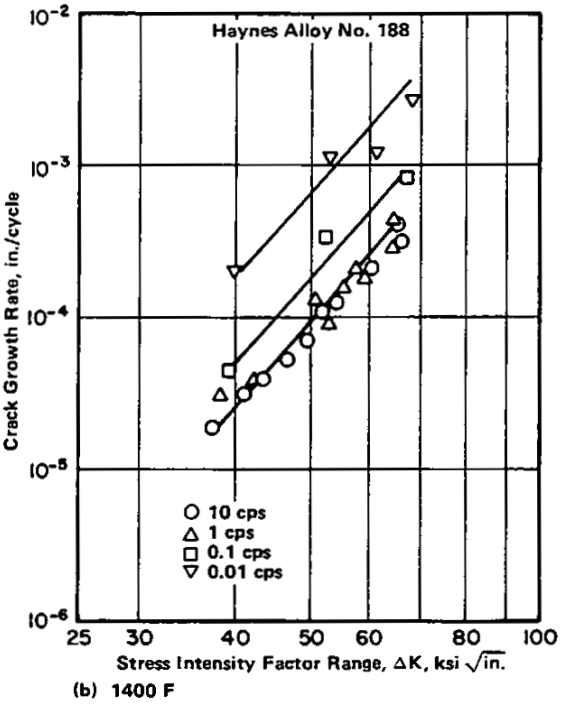

(b) 1400 F

FIGURE 3.056. FATIGUE CRACK GROWTH RATES AT 1110 TO 1600 F (49)

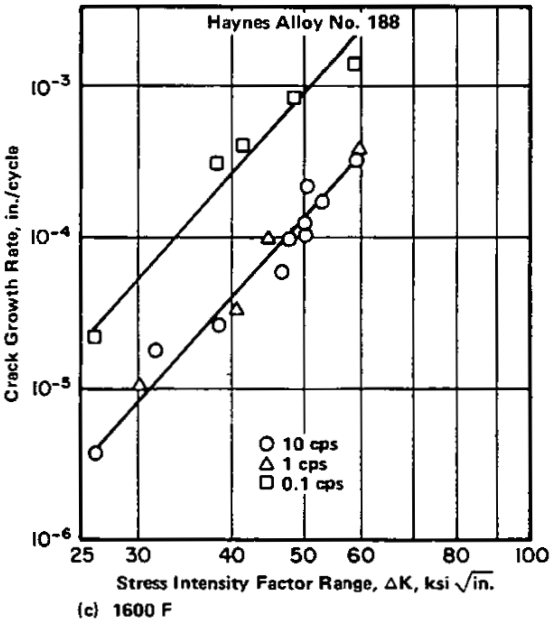

(c) 1600 F

FIGURE 3.056. FATIGUE CRACK GROWTH RATES AT 1110 TO 1600 F (49)

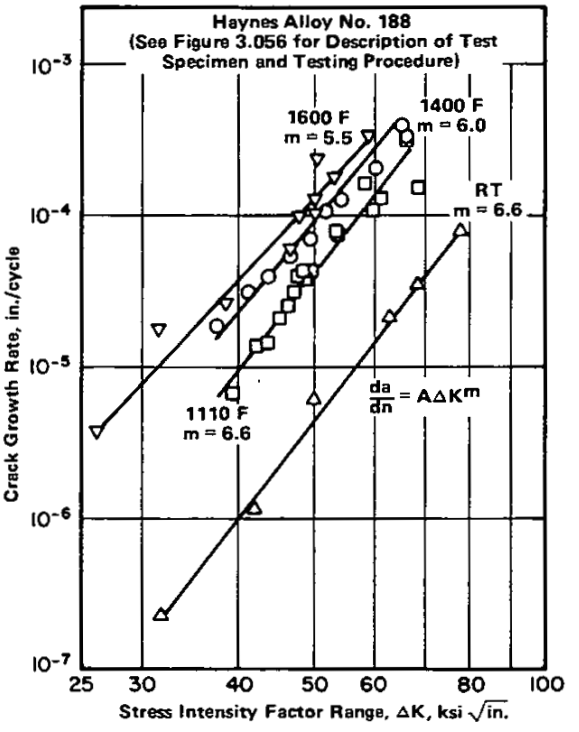

FIGURE 3.057. FATIGUE CRACK-GROWTH RATES AT A FREQUENCY OF 10 CPS AT ROOM TEMPERATURE AND ELEVATED TEMPERATURES (49)

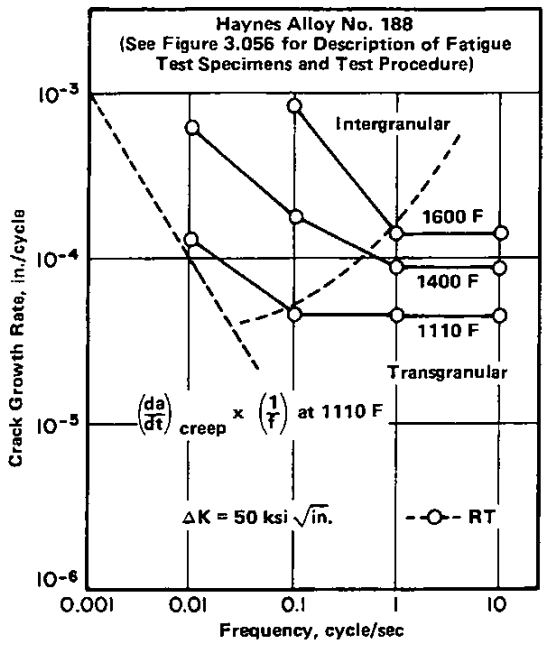

FIGURE 3.058. FREQUENCY AND TEMPERATURE DEPENDENCE OF FATIGUE AND CREEP CRACK-GROWTH RATES (49)

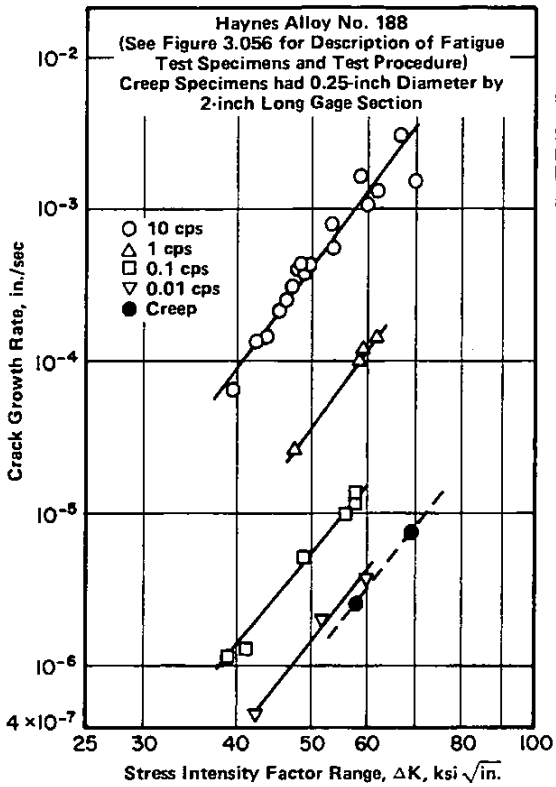

	Co
Low	C
22	Cr
22	Ni
14	W
.08	La

Haynes Alloy No. 188

FIGURE 3.059. CRACK GROWTH PER SECOND AT 1110 F UNDER STEADY STATE CREEP AND UNDER CYCLIC LOADING AT VARIOUS FREQUENCIES (49)

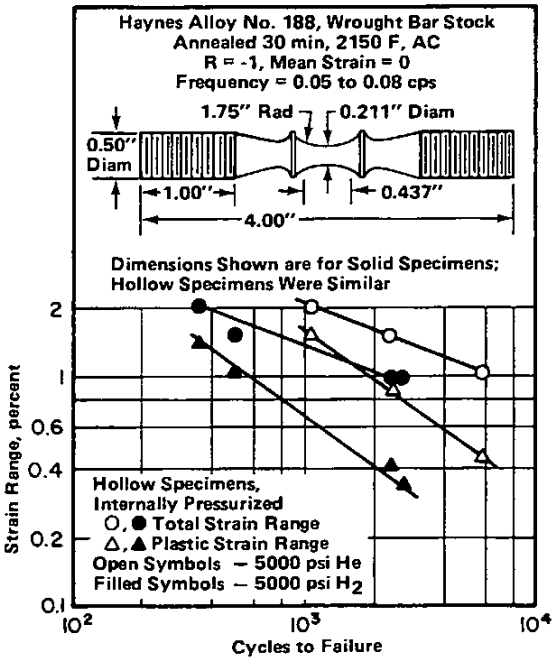

(a) Room Temperature

FIGURE 3.0511. EFFECTS OF HIGH PRESSURE HYDROGEN ON LOW CYCLE FATIGUE LIFE OF HAYNES ALLOY NO. 188 (46,50)

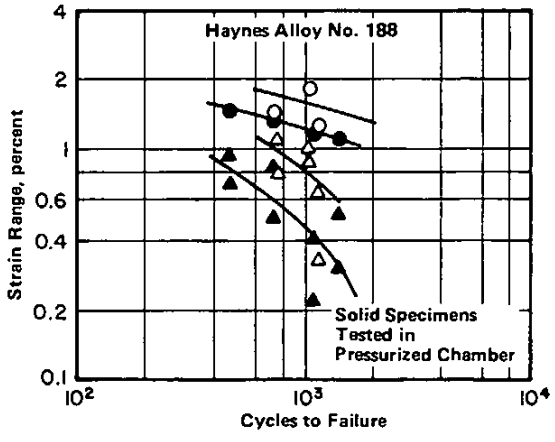

(b) 1250 F

FIGURE 3.0511. EFFECTS OF HIGH PRESSURE HYDROGEN ON LOW CYCLE FATIGUE LIFE OF HAYNES ALLOY NO. 188 (46,50)

	Co
Low	C
22	Cr
22	Ni
14	W
.08	La

Haynes Alloy No. 188

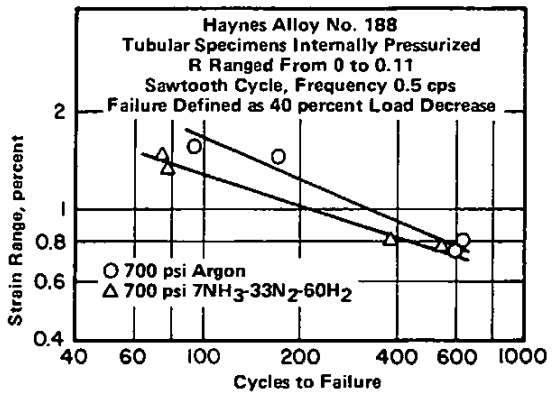

FIGURE 3.0512. EFFECTS OF HYDRAZINE DECOMPOSITION PRODUCTS ON LOW CYCLE COMPRESSIVE FATIGUE AT 1450 F (45)

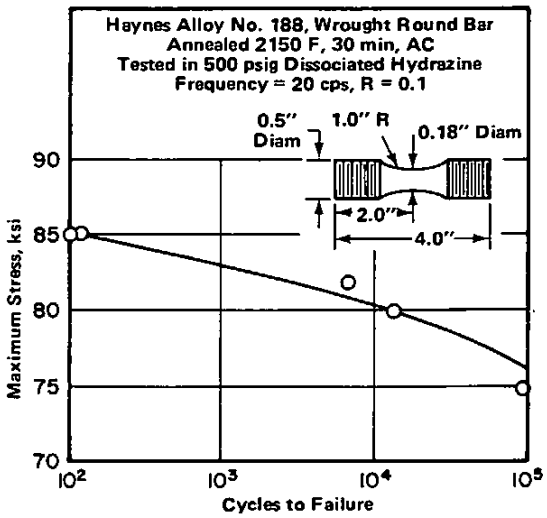

FIGURE 3.0513. HIGH CYCLE FATIGUE STRENGTH OF HAYNES ALLOY NO. 188 AT 1250 F IN HYDRAZINE (46)

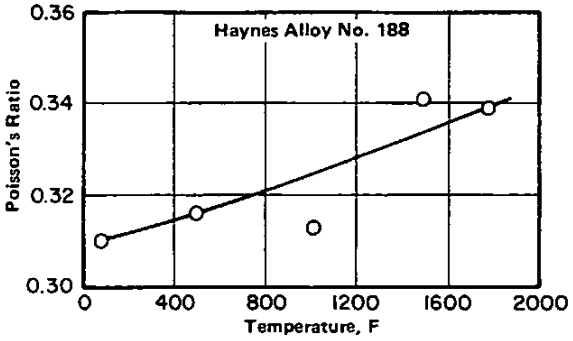

FIGURE 3.061. POISSON'S RATIO (48)

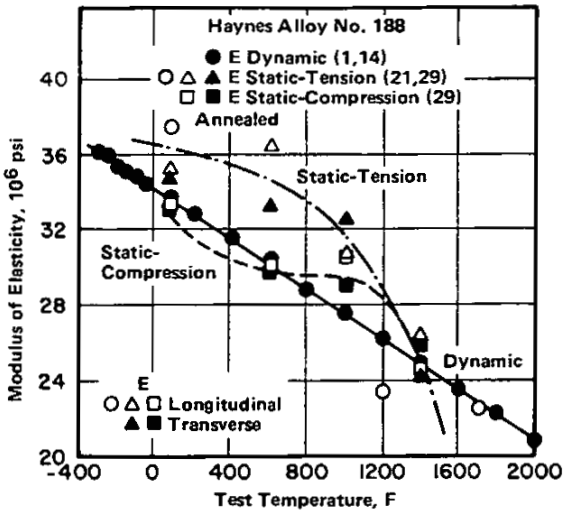

FIGURE 3.062. MODULUS OF ELASTICITY (1,14,21,29)

	Co
Low	C
22	Cr
22	Ni
14	W
.08	La

Haynes Alloy No. 188

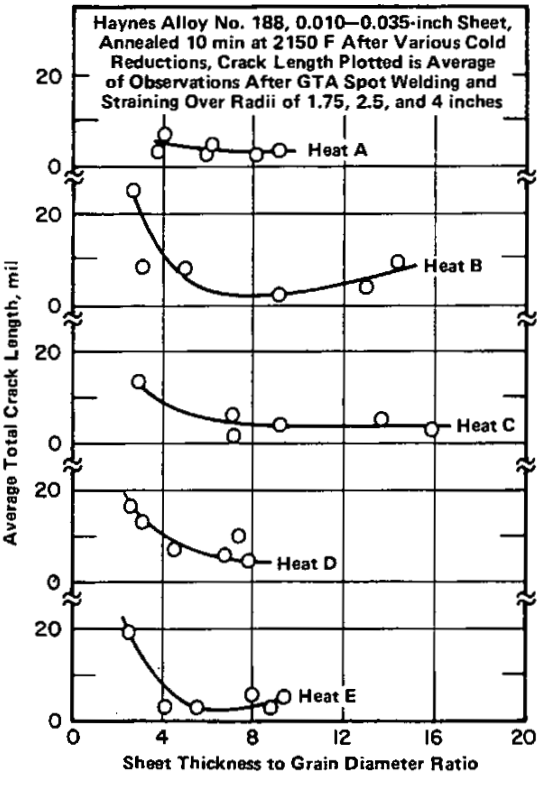

FIGURE 4.036. EFFECT OF SHEET THICKNESS TO GRAIN DIAMETER RATIO ON HOT CRACK SENSITIVITY OF GTA-WELDED THIN GAGE ALLOY FROM FIVE HEATS (51)

	Co
Low	C
22	Cr
22	Ni
14	W
.08	La

Haynes Alloy No. 188

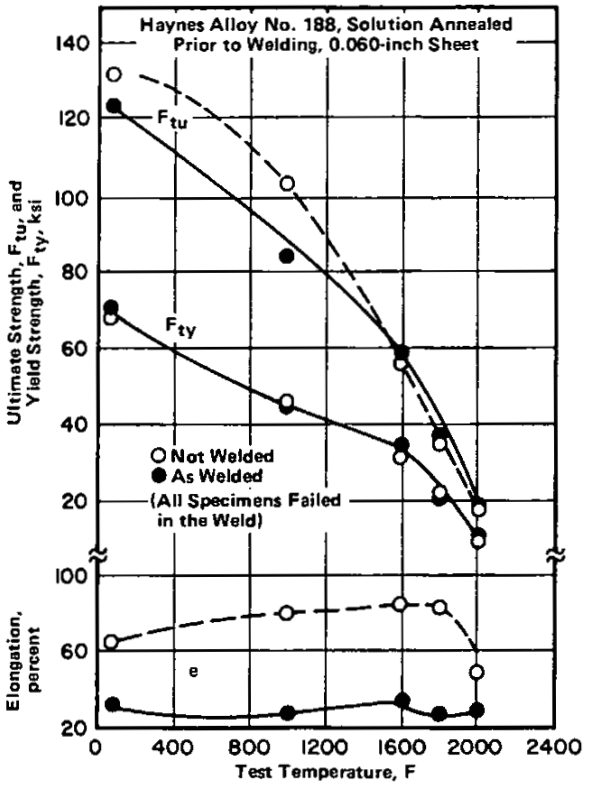

FIGURE 4.039. EFFECT OF TEST TEMPERATURE ON TENSILE PROPERTIES OF GTA-WELDED SHEET (1,16)

Alloy	Haynes Alloy No. 188	
Form	Sheet	
Thickness, in.	0.060	
Condition	Solution Annealed + GTA-Welded	Solution Annealed – Unwelded
Rupture Life, hr at 1500 F - 24 ksi	94.4 (28)	61* (36)**
Rupture Life, hr at 2000 F - 3.2 ksi	28.5 (7)	21* 21**

( ) denotes elongation values.
* Typical—taken from Larson-Miller Parameter curve.
** Typical elongation.

TABLE 4.0310. RUPTURE LIFE OF GTA-WELDED SHEET (1,16)